Pro gradu -tutkielma
Teoreettinen fysiikka

The gradient expansion and topological insulators

Jukka Väyrynen
2011

Ohjaaja: TkT Teemu Ojanen
Tarkastajat: TkT Teemu Ojanen
prof. Kari Rummukainen

HELSINGIN YLIOPISTO
FYSIIKAN LAITOS

PL 64 (Gustaf Hällströmin katu 2)
00014 Helsingin yliopisto

HELSINGIN YLIOPISTO — HELSINGFORS UNIVERSITET — UNIVERSITY OF HELSINKI

Tiedekunta/Osasto — Fakultet/Sektion — Faculty	Laitos — Institution — Department
Faculty of Science	Department of Physics

Tekijä — Författare — Author
Jukka Väyrynen

Työn nimi — Arbetets titel — Title

The gradient expansion and topological insulators

Oppiaine — Läroämne — Subject
Theoretical physics

Työn laji — Arbetets art — Level	Aika — Datum — Month and year	Sivumäärä — Sidoantal — Number of pages
M.Sc. thesis	March 2011	68

Tiivistelmä — Referat — Abstract

Topological insulators are the fastest growing topic in contemporary condensed matter physics. In this thesis we present a novel microscopic method to investigate the properties of these new phases of matter. This method is a gradient expansion of the effective action. We re-derive previously known results and present a number of new ones. Open problems and future directions are also discussed.

Topological insulators are recently discovered extraordinary materials with peculiar band structure properties making them interesting from standpoints of both applications as well as basic research. These materials are insulating in the bulk but have a surface which is a special kind of helical metal. The surface electrons are in a topologically protected conducting state, similar to the edge modes in an integer quantum Hall state. The integer quantum Hall system is described by a quantized conductance which is the response of the electrons to an external electric field. The conductance is a topological invariant showing up as the coefficient of a Chern-Simons electromagnetic action. Similar electromagnetic responses also describe topological insulators but finding the corresponding topological invariants can be difficult. This is where the gradient expansion method comes in.

The gradient expansion is a widely used technique to simplify kinetic equations in transport theory. The method is applicable when there are two different length scales in the studied problem – the physical idea is a well-defined separation of these scales. We show how to utilize this method in a different problem: extraction of topological terms from an effective action. Besides obtaining the previously known topological terms, we show that the gradient expansion can be used to discuss solitons in topological media. We use the method to investigate domain walls or textures in two- and three-dimensional topological insulators. In three dimensions we obtain a half-integer quantized Hall conductance on the texture plane and in two dimensions we generalize the charge fractionalization result of Jackiw and Rebbi in the boundary of the insulator.

Avainsanat — Nyckelord — Keywords
Topological insulators, Topological phases (quantum mechanics), Quantum Hall effects

Säilytyspaikka — Förvaringsställe — Where deposited

Muita tietoja — övriga uppgifter — Additional information

Preface

This thesis was written in the Low Temperature Laboratory of Aalto University during fall–winter 2010–2011, and it marks the end of my time as a student in the University of Helsinki between 2009 and 2011. Discussions with numerous people have guided me during this period.

I am indebted to my thesis advisor Teemu Ojanen, who is both smart and most humorous person to work with and has taught me a lot about physics, research and writing. I am also grateful to Grisha Volovik for collaboration and patiently explaining so much physics to me. I also acknowledge Tero Heikkilä for hiring me in the first place and allowing me to work on my thesis full-time paid. I want to thank University of Helsinki faculty Esko Keski-Vakkuri, Claus Montonen and Kari Rummukainen for reviewing and commenting the thesis and for doing it swiftly. Special thank you to Oona Kupiainen, Tuukka Meriniemi, Joni Suorsa and Jussi Määttä for commenting the introductory section of the manuscript. I am particularly thankful to Jussi for taking the time to teach me so much English grammar. Thank you also to Kumpula campus library for acquiring the two books I needed in my research.

A big thank you to my friends and colleagues in University of Helsinki and Aalto University: you have made the past year and a half an exciting and pleasant period in my life. I am also very grateful for my teachers Esko Keski-Vakkuri and Erkki Thuneberg for valuable career discussions and encouragement.

Finally, I would like to thank my family who have always encouraged me to follow my own aspiration, and nonetheless been supportive and interested in what I do.

Jukka Väyrynen, Otaniemi 12.4.2011

0.1 Conventions

Throughout this thesis we set $c = \hbar = a = 1$, $E_F = 0$ where a is the lattice constant and E_F the Fermi energy. Thus all (crystal) momenta will be dimensionless and 2π-periodic, the one-dimensional Brillouin zone is $[-\pi, \pi]$. We work in $(d+1)$ dimensional space-time and follow the conventional notation dD referring to the spatial dimension only. Spatial dD vectors will be written with boldface, $\mathbf{A} = (A_1, \ldots, A_d)$. We sum over repeated indices. Spatial indices are denoted with Latin letters, $\mathbf{A} \cdot \mathbf{B} = A_i B_i$, $i = 1, \ldots, d$. Greek letters are used with space-time indices, $A \cdot B \equiv A_\mu B^\mu = A_0 B_0 - \mathbf{A} \cdot \mathbf{B}$, $\mu = 0, 1, \ldots, d$ and $(d+1)$ dimensional vectors are denoted $A = (A_0, \mathbf{A})$. In particular, $k = (\omega, \mathbf{k})$ is the notation for frequency-momentum four-vector.

Three kinds of traces are seen in this thesis. The lower-case tr denotes trace over matrix indices. Capitalization, Tr, is used in two cases depending on the operator we trace over. For Wigner transformed operators (the vast majority in this thesis) we define

$$\mathrm{Tr}\, A_W \equiv \int d^{d+1}X \int \frac{d^{d+1}k}{(2\pi)^{d+1}} \mathrm{tr}\, A_W(X,k)$$

and for normal operators

$$\mathrm{Tr}\, A \equiv \int d^{d+1}x_1 \mathrm{tr}\, A(x_1, x_1).$$

Some symbols are explained below:

A	electromagnetic four-potential, $A = (A_0, \mathbf{A})$
$\mathcal{A}$	Berry's phase gauge field
$[A, B]_+$	anticommutator, $[A, B]_+ = AB + BA$
e	unit charge, $e > 0$
$\varepsilon^{\alpha\beta\gamma\ldots}$	Levi-Civita symbol
$\equiv$	definition
E_F	Fermi energy $E_F = 0$
$f_{[i_1 i_2 \ldots i_n]}$	antisymmetrization, $f_{[i_1 i_2 \ldots i_n]} \equiv \frac{1}{n!} \sum_{S_n} (-1)^P f_{P i_1 P i_2 \ldots P i_n}$
$\gamma_{0,1,2,3}$	4×4 Euclidean gamma or Dirac matrices

γ_5	$\gamma_5 \equiv \gamma_0\gamma_1\gamma_2\gamma_3$, the fifth gamma matrix
G	Matsubara Green's function, see Appendix B
$\mathcal{G}$, G_W	Wigner transformed Green's function, see Appendix C
h	Planck's constant
Λ_α	$\Lambda_\alpha \equiv \mathcal{G}_0\partial_\alpha\mathcal{G}_0^{-1}$
$\sigma_{1,2,3}$, $\tau_{1,2,3}$	2×2 Pauli matrices, also $\sigma_{x,y,z}$, $\tau_{x,y,z}$
$\sigma_\pm$	$\sigma_\pm \equiv (\sigma_1 \pm i\sigma_2)/2$
T_τ	time-ordering operator
$\mathbb{Z}_2$	the group of two elements
$2\mathbb{Z}$	the group of even integers

Contents

Chapter 1

Introduction

Topology is an area of mathematics that classifies geometrical objects according to their general properties that are preserved under smooth deformations. Well-known examples are a donut (a torus) and a coffee cup which are topologically the same because they can be smoothly deformed into one another without tearing the surface. On the other hand, a torus is different from a sphere because they cannot be smoothly morphed into one another. The two are said to belong to different topological equivalence classes. The property that separates topological classes is called a topological invariant. In the case of closed two-dimensional (2D) surfaces, such as a torus or a sphere, the invariant is the number of handles in them and called the *genus*.

Topology is not a mere mathematical construction, but is also widely encountered and employed in physics. In condensed matter physics one can find topological invariants for quantum systems, just like for 2D surfaces we have the genus. These kind of *topologically ordered* phases can be seen in both non-interacting and interacting systems [1, 2]. In this thesis we discuss only the first case, i.e., non-interacting systems from a single-particle point of view. The interacting case remains open, see the end of Sec. 1.1.

The topological invariants in condensed matter systems describe the quantum-mechanical wave functions in the Hilbert space. In *gapped systems* there is a finite energy gap separating the ground state (valence band in insulators) from the excited states (conduction band), examples of such phases of matter are insulators and superconductors. For these systems a smooth deformation is defined to be one that does not close the gap and is *adiabatic*[1]. We emphasize that temperature can change the notion of smoothness and topology in the system: if the energy gap is smaller than the typical scale of thermal

[1] Adiabaticity means that the system remains in its ground state during the process.

excitations, the system cannot be considered gapped anymore. Therefore we will work at zero temperature in this thesis. Obviously, our definition of topology cannot be applied to gapless systems such as metals. Gapless systems will not be discussed in this thesis.

Nevertheless, gapless states are what makes topological quantum matter interesting. From topology it follows that if two topologically distinct gapped systems are put next to each other, there must exist a gapless mode in the interface separating the two. Namely, the topological invariant must change somewhere in between and because it cannot by definition change smoothly, the gap has to close. This means that two insulators belonging to different topological classes will have a common conducting boundary. Moreover, the conducting properties of the boundary can be very different from ordinary metals. Therefore, an insulator which cannot be adiabatically connected to the vacuum (which is also an insulator) will have conducting surface. Such an insulator is called a *topological insulator* (TI, coined by Moore and Balents [3]) whereas the vacuum is a *trivial* insulator.

The topological invariants describing these exotic systems are most often $\mathbb{Z}_2$- or $\mathbb{Z}$-valued. For example, the integer quantum Hall (IQH) state has a $\mathbb{Z}$ invariant whereas the recently discovered time-reversal invariant (TRI) topological insulators based on the spin-orbit interaction (SOI) are classified with $\mathbb{Z}_2$ invariants. There are two ways of looking at topological phases: the effective field theory (EFT) way and the band theory (BT) way. The BT picture was successfully used in discovering the $\mathbb{Z}_2$ topological insulators in 2005 and 2006. Nonetheless, in this thesis the emphasis is on the EFT approach and on the $\mathbb{Z}$-valued winding number invariants which turn up in the effective field theories. The FT approach to topological insulators is favorable because it immediately gives the electromagnetic responses[2] of the system and also provides hints to discuss interacting systems. Besides, the FT can be used to explain the $\mathbb{Z}_2$ invariants through a dimensional reduction procedure [5].

The purpose of this thesis is twofold. We describe the *gradient expansion* method which is a novel technique in the study of topological phases. We will review the basic theory of topological insulators with emphasis on the FT description, and on the way derive some previously known and unknown results with our gradient expansion tool.

This thesis is organized as follows. In Section 1.1 we explain from a historical standpoint how topological insulators were discovered and what they are. We will mostly focus on the 2D $\mathbb{Z}_2$ insulator but also discuss the 3D insulators. The emphasis is on the BT picture but later in this thesis we will be FT oriented. In Sections 1.2 and 1.3 we

[2]Also other kinds of responses, such as thermal or magnetic dipole responses have been discussed [4].

introduce the Berry phase and explain the topology of the integer quantum Hall effect (IQHE). We will also show how the IQH effective action is obtained from the gradient expansion. In Chapter 2 we introduce the so-called periodic table of topological phases of matter. We also derive a result concerning the evaluation of a certain topological invariant. In the end of the chapter, we introduce the essence of the FT approach, the dimensional reduction and the 4D Chern-Simons (CS) FT. We will also obtain the latter with the gradient expansion method. In Chapter 3 we discuss solitons in topological media. With the gradient expansion we derive and evaluate topological invariants for mass domain walls in 3D and 1D. Finally, in Chapter 4 we draw the conclusions and discuss future directions. The three appendices contain essential technical details not suitable to be presented in the main text. In the first, we derive the Hall conductance with the Kubo formula. In the second appendix, we derive the zero temperature effective action from the fermionic single-particle path integral. Finally, in Appendix C, the gradient expansion is thoroughly examined and motivated. Even though the gradient expansion is an essential and perhaps the most important ingredient of this thesis, we have decided to present it in an appendix rather than as a part of the main text. The reason for this is to maintain the coherence and readability of the main text, but also keep the discussion on physics rather than on mathematical methods – even if physically motivated such as the gradient expansion.

1.1 Historical overview and motivation

In this section we give a short historical introduction to topological insulators. We base this section on the three review articles by Hasan and Kane [6], Hasan and Moore [7] and Qi and Zhang [8]. In the end we briefly explain why these recently discovered materials are of interest to physicists and what are the open questions in the subject from a theoretical point of view.

Topological classification of phases of matter started already in the 1970s when superfluid helium and liquid crystals were studied from the standpoint of the so-called Landau symmetry breaking paradigm [9, 10, 11]. The classification is based on homotopy theory and the invariants are presented as real space integrals involving the order parameter field of the system. One speaks of real space topology and we will return to this later in Chapter 3.

A novel topologically ordered phase which did not fit into this symmetry break-

ing paradigm was discovered in 1980 in a 2D electron gas in a perpendicular magnetic field [12]. This is the the quantum Hall effect and it was first theoretically explained by Laughlin [13]. The QH state will be discussed in more detail in the next section. In short, one can calculate the band structure for the QH system and see that it is gapped or insulating. Despite this, the QH slab is conducting with quantized conductance. The QH states are labeled by a topological invariant [14, 15] called the *TKNN invariant* after Thouless, Kohmoto, Nightingale and den Nijs [1]. This invariant can be expressed as a Chern number which is an integral in momentum space. The $\mathbb{Z}$-valued TKNN invariant is the conductance in units of the conductance quantum e^2/h. Interestingly, the charge is transferred only along the edges and the edge modes are robust to disorder [13]. The robustness is explained by the topological invariance of the conductance and the edge modes are said to be *topologically protected*. In an interacting system, the *fractional quantum Hall state*, the conductance can have fractional values.

It took over 20 years before the next big discovery in non-interacting systems was made. In 2005, Kane and Mele published two seminal papers introducing 2D topological insulators [16, 17]. In Ref. [17] the authors discuss effects of spin-orbit interaction (SOI) in graphene. They show that including a SO term in the Hamiltonian opens a gap and moves the system to a novel insulating state which cannot be adiabatically connected to a normal insulator. This new topologically ordered state is called the quantum spin Hall (QSH) state and it resembles the QH state although in this case time-reversal symmetry (TRS) is not broken and no external magnetic field is needed. Intuitively, the up and down-spin electrons are separately in QH states experiencing opposite effective magnetic fields due to the SOI [3]. This defines a topological invariant in terms of $n_\uparrow - n_\downarrow$ which is the difference between the TKNN invariants of the two spin states. Furthermore, Kane and Mele show that the QSH state supports gapless edge modes which are *helical*, i.e., their spin is fully correlated with the propagation direction. Similar to the IQHE, these modes are protected by topology. However, in this case the protection is because of TRS and leads to a $\mathbb{Z}_2$ invariant so that the number of protected edge modes is defined only "modulo 2". In the case of only one edge channel, the two spin states cannot elastically backscatter to each other because of TRS[3]. This prevents Anderson localization even in the presence of strong disorder. On the other hand, if there are two TRI edge channels (four states) then backscattering is allowed from one channel to another, leading to localization and resistance. In this sense "two equals zero" where "zero" means the trivial

[3]At finite temperature inelastic backscattering is allowed.

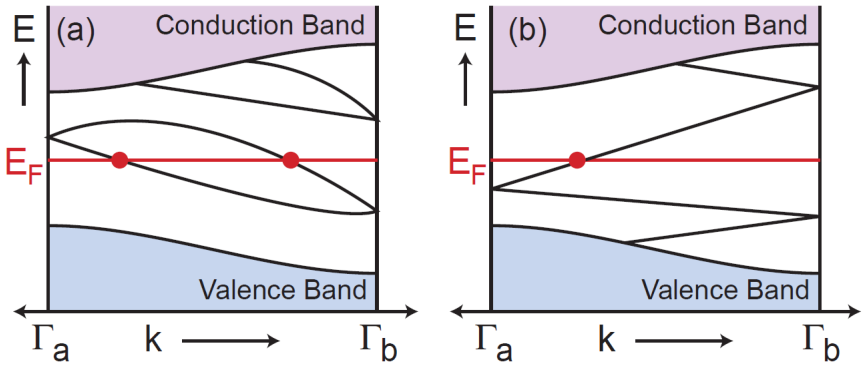

Figure 1.1: Half of the 1D Brillouin zone (BZ) for the momentum k along a boundary. A trivial insulator (a) and a topological insulator (b) band structures are shown. Because of TRS, the BZ is symmetric around the point $\Gamma_a = 0$. According to Kramers' theorem, the states have to be twice degenerate at the TR invariant momenta Γ_a, $\Gamma_b = -\Gamma_b$. Elsewhere, the degeneracy is lifted by the SOI. There are two ways to pair the states at Γ_a to those at Γ_b. The topologically trivial way always intersects the Fermi energy E_F an even number of times in the half BZ, whereas for the TI this number is odd. The slope of the dispersion in the crossing gives velocity of the edge state. The figure is taken from Ref. [6].

insulating phase. Likewise one can consider many edge channels and conclude that the phases have a parity which is the $\mathbb{Z}_2$ topological invariant. If TRS is broken on the edge, the edge states will become gapped, see Sec. 3.3.

Judging from the above description it would seem that the QSH state requires S_z (defining 'up' and 'down' spins) to be conserved, and thus this phase would be just a finely tuned abnormality never encountered in nature. In fact, a state of matter similar to the QSH insulator was proposed already in 1989 in thin ^{3}He films [18, 19]. The major breakthrough by Kane and Mele was to show that the new phase of matter is actually stable. In the second paper, Kane and Mele showed that the QSH state in graphene is robust even to S_z non-conserving perturbations [16]. They also derive a $\mathbb{Z}_2$ topological invariant which does not rely on S_z conservation. This invariant classifies the phases and is calculable directly from the band structure. The invariant can be understood pictorially by thinking about the Kramers' pairs in the dispersion of the edge states as shown in Fig. 1.1.

Unfortunately, graphene has a weak SOI because it is made out of carbon which is a

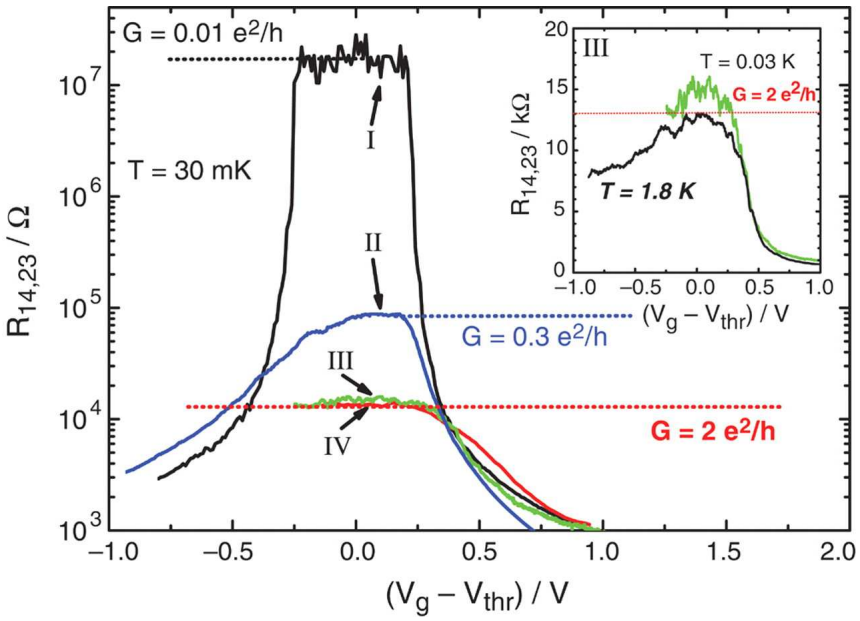

Figure 1.2: The longitudinal four-terminal resistance and conductance G shown for normal (I, $d = 5.5\,\mathrm{nm}$) and inverted (II–IV, $d = 7.3\,\mathrm{nm}$) band structures in zero magnetic field and temperature of 30 mK. Apart from the thickness d, the device size is the same in I and II and different in II–IV. The horizontal axis essentially shows the Fermi level position. When the Fermi level goes to the band gap, the normal insulator (I) shows strong resistance reaching the detection limit of about $10\,\mathrm{M\Omega}$ of the experimental equipment. The QSH state (II–IV) shows the predicted conductance. The sample II is 20 times longer than III and IV, whose length is $1\,\mu\mathrm{m}$. The elastic mean free path is estimated to be a few microns and therefore the reduced conductance of sample II is attributed to inelastic backscattering [8]. The samples III and IV differ in their widths but nevertheless show the same resistance, indicating that the charge is transported along the edges only. The picture is taken from Ref. [21].

light element. In graphene the gap predicted by Kane and Mele is small and the QSH effect would be very difficult to observe. A resolution came in 2006, when Bernevig, Hughes and Zhang proposed the QSH state in a quantum well consisting of a HgTe layer between CdTe [20]. Both of these materials are semiconductors and the authors showed that when the thickness of the HgTe layer exceeds a critical value of $d_c = 6.3\,\mathrm{nm}$ a band-inversion happens in the HgTe, signaling a quantum phase transition between a trivial insulating phase and the QSH phase. In the following year the QSH phase in HgTe was observed in a transport experiment, Fig. 1.2 [21].

The next important step was the generalization of the Kane-Mele $\mathbb{Z}_2$ invariant to 3D. This was done independently by Moore and Balents [3], Fu and Kane [22], and Roy [23]

in 2006. Also the 3D TI is based on the SOI and has a conducting surface. In the spirit of the 2D TI, it is worthwhile to investigate the four TR invariant momenta of the surface Brillouin zone (BZ). These TRI momenta can be connected similarly to Fig. 1.1 and the corresponding $\mathbb{Z}_2$ invariants can be calculated. It turns out that there are four $\mathbb{Z}_2$ invariants and 16 different phases. Some of these are in a "weak topological insulator" phase where there are gapless surface modes but they are not protected by topology as in the 2D QSH system. The weak TI can be understood as a stack of 2D QSH insulators. The remaining phases are the ones that cannot be obtained from the 2D insulators. They are called the "strong topological insulators". These have an odd number of Kramers degenerate Dirac cones inside the surface Fermi-arc[4]. The surface of a strong TI is thus similar to graphene which has four Dirac cones. However, there are differences with important consequences. The surface modes of a 3D TI cannot be localized by disorder, similarly to the protection of the QSH edge states. Likewise, also the 3D TI surface states are spin-polarized. Also, a TRS breaking perturbation on the surface makes it fully insulating and gives rise to interesting phenomena. Even if the TRS breaking is small, there will be a half-integer QHE on the surface [22, 5], see Sec. 2.4 and the 1D counterpart in Sec. 3.10. More interesting is the *topological magnetoelectric effect* (TME) which realizes the axion electrodynamics proposed in field theory [25]. Both are still lacking experimental confirmation and observation of the former might even be inaccessible [26]. There is high expectations on the TME which could be used to observe such effects as a point charge induced image magnetic monopole[5] [27] or the Witten effect [28].

Candidate materials for the 3D strong TI were proposed later in 2006 [26]. The massless Dirac spectrum and spin polarization of the surface states were soon observed in the proposed semiconducting alloy $Bi_{1-x}Sb_x$ (for certain range of x) [29]. A "second generation" of topological insulating materials such as Bi_2Te_3, Bi_2Se_3 and Sb_2Te_3, were proposed and experimentally confirmed in 2009 [30, 31, 32, 33, 34]. These materials have simpler surface states and a larger band gap than $Bi_{1-x}Sb_x$. Perhaps the most important is the Bi_2Se_3 which has many desirable properties and a band gap of roughly 3600K making it truly a room-temperature TI. The famous Dirac cone structure observed with angle resolved photoemission spectroscopy (ARPES) is shown in Fig. 1.3 [31]. The spin helicity of the surface states was also observed.

[4]These Dirac cones have their time-reversal partners on the opposite surface of the sample. This is dictated by the Fermion doubling theorem [24].

[5]Or rather a *dyon* since this monopole has also an induced electron charge.

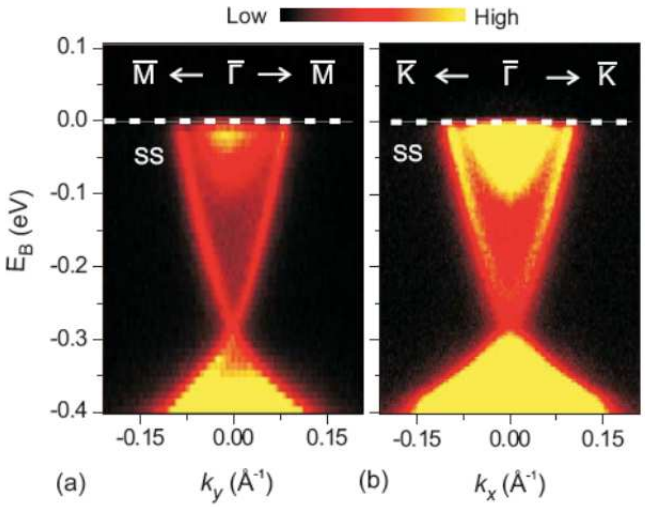

Figure 1.3: An ARPES measurement showing the Dirac cone in the electronic dispersion on the surface of the strong TI Bi_2Se_3. The color shows the density of states and the white dotted line denotes the Fermi energy. The picture is taken from Ref. [31].

Some basic research motivation to study topological insulators was already mentioned above. An important phenomenon from the quantum computing perspective is how the superconducting proximity effect influences the gapless surface modes of a 3D TI. When a superconductor is placed next to a TI, a vortex in the superconductor can induce a *Majorana fermion* on the TI surface [35, 36, 37]. Majorana fermions are peculiar hypothetical particles predicted theoretically over 70 years ago but still lacking experimental confirmation [38]. These particles are their own antiparticles and in 2D obey non-Abelian statistics, making them candidates for topological quantum computation [39]. Of course the dissipationless and spin-polarized transport properties of topological insulators make them interesting also for engineering applications, e.g., *spintronics*.

The open theoretical problems in the field concern interacting systems where the band theory characterization does not work. The discussions above have all treated non-interacting electrons and *Thouless-type* topological order where the topological invariant manifests in the response of the system. An example is the IQH state where the electronic response is determined by the topological invariant, the Hall conductivity. On the other hand, the interacting, fractional QH state is characterized with a *Wen-type* topological order and described by a topological field theory [2]. Identifying the Wen-type order and fractional topological insulators [40] is an unsolved problem in the field, although some advancement has been made with different approaches [41, 42, 43, 4].

1.2 Berry's phase

In this section, we introduce the general idea of the Berry phase which is helpful in understanding topological properties and classification of condensed matter systems. The Berry phase also serves as an example of how topological invariants can be evaluated. We will briefly have to expose the reader to the highly abstract mathematical concept of fiber bundles and connections on fiber bundles. In this, we will follow the treatment of Nakahara [44]. In Section 1.2 we will make the discussions concrete by using our methodology to explain the IQHE – our first example of a topological insulator.

Let us start by considering a Hamiltonian $H(\mathbf{R})$ depending on k parameters denoted by a k-vector $\mathbf{R} = (R_1, \ldots, R_k) \in M$, living on a parameter manifold M. In this thesis M will always be the Brillouin zone. Let $\{|n, \mathbf{R}\rangle\}$ be a normalized eigenbasis of the Hamiltonian, $H(\mathbf{R})\,|n, \mathbf{R}\rangle = E_n(\mathbf{R})\,|n, \mathbf{R}\rangle$. Consider now an adiabatic time-evolution of the vector $\mathbf{R}$. Due to the adiabaticity, the system remains in the same state but gains a phase factor [45]:

$$|n, \mathbf{R}(t_0)\rangle \to e^{i\theta_n(t)}\,|n, \mathbf{R}(t)\rangle\,.$$

The phase θ_n is determined by the time-dependent Schrödinger equation, the result is

$$\theta_n(t) = -\int_{t_0}^{t} dt' E_n(\mathbf{R}(t')) + i\int_{t_0}^{t} dt'\,\langle n, \mathbf{R}(t')|\,\nabla\,|n, \mathbf{R}(t')\rangle \cdot \frac{d}{dt'}\mathbf{R}(t').$$

The first term is the familiar dynamical time-evolution while the second term is known as the *Berry phase* η_n:

$$\eta_n(R(t)) = i\int_{\mathbf{R}_0}^{\mathbf{R}} dR'^i\,\langle n, \mathbf{R}'|\,\frac{\partial}{\partial R'^i}\,|n, \mathbf{R}'\rangle \tag{1.1}$$

where $\mathbf{R} \equiv \mathbf{R}(t)$, $\mathbf{R}_0 \equiv \mathbf{R}(t_0)$. Note that η_n is indeed real since $\langle n, \mathbf{R}|\,\partial_i\,|n, \mathbf{R}\rangle = -(\partial_i\,\langle n, \mathbf{R}|)\,|n, \mathbf{R}\rangle$.

This all gets more interesting when one looks at the phase freedom of quantum mechanics, which is a symmetry in each parameter configuration $R \in M$. In mathematical terms, the phase freedom is a local (in M) U(1) symmetry of the quantum mechanical system. We are thus interested in the properties of a manifold M with an associated Lie group in each point. The mathematical framework to discuss such objects is the theory of fiber bundles. We are, however, only interested in the so-called principal bundles. In

short, a principal bundle $P(M,G)$[6] is a mathematical object consisting of a base manifold M, a Lie group G, and transition functions to move from one coordinate patch to another on the base manifold. Additionally, $P(M,G)$ is locally isomorphic to $M \times G$ while the transition functions contain the global topological structure of the principal bundle.

Fiber bundles can be classified according to their topological properties and these classifications can be given by integrals of the bundle curvature, the so-called Chern numbers. These integrals are integer-valued and topological invariants similar to that of the Gauss-Bonnet theorem of 2D surfaces [44]. The Gauss-Bonnet theorem states that the integral of the Gaussian curvature over a 2D manifold is quantized to the number of handles of the manifold[7]. To obtain the curvature on a fiber bundle, a connection has to be defined on it. Connections on principal bundles are abstract objects presented as 1-forms with no explicit relationship to the connections used in, for example, general relativity. However, in the end the connection describes the same thing as in Riemannian geometry: means to parallel transport vectors.

We will next use the Berry phase as an example of a U(1) bundle, but the results we obtain are easily generalized. We investigate the U(1) principal bundle $P(M,U(1))$ over the parameter manifold M. As discussed above, to investigate the topological properties, we have to introduce a connection to obtain the curvature from it. One can show that a particular connection on $P(M,U(1))$ is given by the 1-form

$$\mathcal{A}^{(n)}(R) = \langle n,\mathbf{R}|\,\partial_i\,|n,\mathbf{R}\rangle\,dR^i \equiv \langle n,\mathbf{R}|\,d\,|n,\mathbf{R}\rangle\,, \tag{1.2}$$

where the last term is written with the exterior derivative d. We often omit the indices (n,R) in the connection, and write simply $\mathcal{A}$. A U(1) transformation of the states leads to the following gauge symmetry of the field $\mathcal{A}$:

$$|n,\mathbf{R}\rangle \to e^{i\chi(\mathbf{R})}\,|n,\mathbf{R}\rangle$$
$$\mathcal{A} \to \mathcal{A} + id\chi.$$

Writing $\hat{\mathcal{A}}_i \equiv \langle n,\mathbf{R}|\,\partial_i\,|n,\mathbf{R}\rangle$, we see that they are components of a U(1) gauge field [46]. In general this field need not to be an Abelian gauge field. We could also define a non-Abelian connection

$$\mathcal{A}^{nm}(\mathbf{R}) = \langle n,\mathbf{R}|\,d\,|m,\mathbf{R}\rangle\,,$$

[6] Read: G bundle over M.

[7] This is strictly true only for manifolds without boundaries. If the manifold is not closed, i.e., it contains *holes*, these holes will give additional quantized boundary contribution to the invariant.

in which case the commutator $[\hat{\mathcal{A}}_i, \hat{\mathcal{A}}_j]$ need not vanish. Keeping this in mind, we define the curvature generally as

$$\mathcal{F} \equiv d\mathcal{A} + \mathcal{A} \wedge \mathcal{A} = \left(\partial_i \hat{\mathcal{A}}_j + \hat{\mathcal{A}}_i \hat{\mathcal{A}}_j\right) dR^i \wedge dR^j. \tag{1.3}$$

This is sometimes also called the field strength in analogy to electromagnetism.

Now we are ready to introduce the topological invariants. First, we introduce 2-forms called Chern characters. For our purposes it is enough to introduce only the first two of them,

$$\begin{aligned} \mathrm{ch}_1(\mathcal{F}) =& \frac{i}{2\pi} \sum_n \mathcal{F}^{nn} = \frac{i}{2\pi} \sum_n d\mathcal{A}^{nn} && (1.4) \\ \mathrm{ch}_2(\mathcal{F}) =& \frac{-1}{8\pi^2} \sum_n (\mathcal{F} \wedge \mathcal{F})^{nn} \\ =& \frac{-1}{8\pi^2} \sum_n d\left(\mathcal{A} \wedge d\mathcal{A} + \frac{2}{3}\mathcal{A} \wedge \mathcal{A} \wedge \mathcal{A}\right)^{nn}. && (1.5) \end{aligned}$$

We have also written the *locally exact* forms of ch_1 and ch_2. The invariants themselves, the Chern numbers, are integrals of the Chern forms over M:

$$\begin{aligned} C_1(\mathcal{F}) =& \frac{i}{2\pi} \int_M \sum_n \mathcal{F}^{nn} && (1.6) \\ C_2(\mathcal{F}) =& \frac{-1}{8\pi^2} \int_M \sum_n (\mathcal{F} \wedge \mathcal{F})^{nn}. && (1.7) \end{aligned}$$

These are gauge invariant and quantized to integers.

1.3 The integer quantum Hall effect

In this section we discuss the concepts of Section 1.2 in a real-life physical setup. The IQH system is a free 2D electron gas with a TRS breaking perpendicular magnetic field $\nabla \times \mathbf{A}$ penetrating the sample. This system has highly degenerate energy levels called *Landau levels* [45] where the degeneracy is lifted by impurities. Calculating the band structure for the Hamiltonian shows a gap in the bulk. Despite the bulk band gap, the QHE shows a transverse Hall conductance just like in the classical case. The conductance has strange quantum-mechanical properties. Unlike its classical counterpart, the conductance is quantized and it is topologically protected. Furthermore, the IQH state has gapless

edge modes and therefore satisfies our definition of a topological insulator. In Chapter 2 we show that the IQH state is a class A TI and has a $\mathbb{Z}$-invariant. This is because the QH state breaks TRS – the conductance quantization can also be seen without net magnetic field as long as the TRS is broken as explained by Haldane in his celebrated paper [47]. Next, we show the topological nature of the QHE. We calculate the off-diagonal components of the conductivity tensor for the IQH system.

Let us start with the standard Hamiltonian for a non-interacting electron in a magnetic field:

$$H(x,y) = \frac{1}{2m}(\hat{\mathbf{p}} + e\mathbf{A})^2 + U(x,y)$$

where U is a generic lattice potential (including the confining potential) and $\hat{\mathbf{p}} = -i\nabla$. One can define a magnetic unit cell and use Bloch's theorem to define the Bloch wave functions [1]. In this case the Schrödinger equation can be written with the Bloch Hamiltonian

$$\mathcal{H}_{\mathbf{k}}(x,y) = \frac{1}{2m}(-i\nabla + \mathbf{k} + e\mathbf{A})^2 + U(x,y), \tag{1.8}$$

which is most useful for us. The conductivity tensor σ_{ij} is defined through the relation $j_i = \sigma_{ij}E^j$, $i,j = 1,2$ and it is antisymmetric in our case. We are interested in the transverse conductivity which is the off-diagonal component σ_{xy}.

In 2D, transverse *conductance* is identical to transverse *conductivity*. Conductance is current divided by electric potential while conductivity is current *density* divided by electric *field*. Now, in 2D current density relates to current through a *cross* length while electric field is related to potential through a *parallel* length. These two lengths are the same for perpendicular current and potential and do not show in the ratio of the two.

The transverse conductance can be calculated with the standard Kubo formula

$$\sigma_{xy}(\omega) = \frac{e^2}{i\omega}\int \frac{d^2\mathbf{k}}{4\pi^2}\sum_{n,m\neq n} n_F(E_n)\left(\frac{v^x_{nm}v^y_{mn}}{\omega_{mn}-\omega} + \frac{v^y_{nm}v^x_{mn}}{\omega_{mn}+\omega}\right), \tag{1.9}$$

where $\hat{\mathbf{v}} = \hat{\mathbf{p}}/m$ is the single-particle velocity operator, $\omega_{mn} = E_m(\mathbf{k}) - E_n(\mathbf{k})$ and n,m label the bands. We have included a quantum-mechanical derivation of this formula in Appendix A using first order time-dependent perturbation theory.

As also shown in Appendix A, the off-diagonal matrix elements $\mathbf{v}_{nm}$ can be written

in terms of the Hamiltonian (1.8) and Eq. (1.9) becomes [1, 5]

$$\sigma_{xy} = \frac{e^2}{h} i \int \frac{d^2\mathbf{k}}{2\pi} \sum_{n\in \text{occ.}} \sum_{m\in \text{unocc.}} \varepsilon^{ij} \frac{(\partial_{k_i} \mathcal{H}_{\mathbf{k}})_{nm} (\partial_{k_j} \mathcal{H}_{\mathbf{k}})_{mn}}{(E_n - E_m)^2} \tag{1.10}$$

This is the basic formula which gives the Hall conductivity in terms of the Bloch Hamiltonian $\mathcal{H}_{\mathbf{k}}$. Below, we show that the transverse conductance σ_{xy} is quantized in units of the the conductance quantum e^2/h. Moreover, this quantized conductance is a topological invariant independent of material parameters.

1.3.1 Topology of the IQHE

The exact topological nature of the IQH state was shown by Thouless et al. [1] and refined by others [14]. In this subsection we discuss the topology of the IQH system, mostly following the paper by Kohmoto [15]. In the spirit of Section 1.2, we start by defining the momentum space Berry connection. In other words, the parameter manifold M is identified with the 2D BZ, and we are considering a U(1) bundle on it. The connection 1-form and the field strength (Eqs. (1.2), (1.3)) are

$$\begin{aligned} \mathcal{A}^{(n)}(\mathbf{k}) &= \langle n, \mathbf{k}| \, \partial_{k_i} \, |n, \mathbf{k}\rangle \, dk^i = \hat{\mathcal{A}}_i^{(n)} dk^i \\ \mathcal{F}^{(n)}(\mathbf{k}) &= \partial_{k_i} \hat{\mathcal{A}}_j^{(n)} dk^i \wedge dk^j, \end{aligned}$$

where n labels the *occupied* bands. Because the connection is Abelian, the first Chern number for a single band n becomes,

$$\begin{aligned} C_1(\mathcal{F}^{(n)}) =& \frac{i}{2\pi} \int_M \mathcal{F}^{(n)}(\mathbf{k}) \\ =& \frac{i}{2\pi} \int d^2\mathbf{k} \left[(\partial_{k_x} \langle n, \mathbf{k}|) \partial_{k_y} |n, \mathbf{k}\rangle - (\partial_{k_y} \langle n, \mathbf{k}|) \partial_{k_x} |n, \mathbf{k}\rangle \right] \\ =& \frac{1}{2\pi i} \int d^2\mathbf{k} \sum_m \varepsilon^{ij} \langle n, \mathbf{k}|\partial_{k_i}|m, \mathbf{k}\rangle \langle m, \mathbf{k}|\partial_{k_j}|n, \mathbf{k}\rangle \end{aligned}$$

which is the same as the conductance of a single band, Eq. (A.4),

$$\sigma_{xy}^{(n)} = \frac{e^2}{i} \int \frac{d^2\mathbf{k}}{(2\pi)^2} \sum_m \varepsilon^{ij} \langle n, \mathbf{k}|\partial_{k_i}|m, \mathbf{k}\rangle \langle m, \mathbf{k}|\partial_{k_j}|n, \mathbf{k}\rangle.$$

We thus have a relation between the single band first Chern number and the conductance [14]:

$$\sigma_{xy}^{(n)} = \frac{e^2}{h} C_1(\mathcal{F}^{(n)}). \tag{1.11}$$

Equation (1.11) shows that the conductance is quantized in the units of the conductance quantum e^2/h. This integer is given by the first Chern number of the band. A sum over occupied bands gives the total conductance as the first Chern number of Eq. (1.6), in the units of e^2/h. In Sec. 1.2, we took the quantization of C_1 as a mathematical fact and gave no justification for it. Nevertheless, an intuitive rationalization can be found in the paper by Kohmoto [15]. In the paper it is explicitly shown that C_1 is integer-valued for the QH system. In brief, Kohmoto shows that $\sigma_{xy}^{(n)}$ has to be invariant under U(1) gauge transformations of the wave functions. However, the wave functions have nodes in the BZ and thus the phase of the wave functions cannot be smoothly and uniquely defined in the entire BZ – the BZ has to be divided to patches where the phase is well defined [48]. On the boundaries of these patches, the wave function has to remain continuous which gives a condition for C_1 to be an integer.

We showed that a topological invariant called the first Chern number has a direct physical interpretation in the IQH system. Namely, it gives the linear response to an external electric field. One might ask if there are other such invariants for the IQH state, for example the second Chern number C_2. The answer is negative [14]. For example the second Chern number, Eq. (1.7), vanishes identically since it is a 4-form and the dimension of M is only two. Nevertheless, in a *four-dimensional* BZ it is not generally zero – this is the observation made by Zhang and Hu [49].

Before showing how the above results are obtained from the gradient expansion, let us briefly comment on the physical content of the connection 1-form $\mathcal{A}^{(n)}$. In 1D one can define a *polarization* P_1 [50, 51] as the BZ integral,

$$P_1 = \frac{ie}{2\pi} \sum_{n \in \mathrm{occ}} \oint_{-\pi}^{\pi} \mathcal{A}^{(n)}.$$

The polarization is not entirely gauge invariant but has an integer ambiguity: a gauge transformation $\mathcal{A}^{(n)} \to \mathcal{A}^{(n)} + id\chi^{(n)}$ with $\chi^{(n)}(\pi) = \chi^{(n)}(-\pi) - 2\pi m$ adds an integer m to P. This ambiguity is physically justified since the polarization is just the shift of charge away from the lattice sites. In 2D we can define the polarization as a function of the second momentum k_y, $P_1 = P_1(k_y)$ and with the integration over k_x. In this case the

Hall conductivity is a winding number of $P_1(k_y)$ [5, 7]: with a proper gauge choice we can make $\partial_{k_x}\mathcal{A}_y^{(n)}$ single-valued, using this and the locally exact form of Eq. (1.4), we have

$$\begin{aligned} C_1 =& \frac{i}{2\pi}\sum_{n\in\text{occ}}\int_{BZ} d\mathcal{A}^{(n)} \\ =& \oint dk_y \partial_{k_y}\left(\frac{i}{2\pi}\sum_{n\in\text{occ}}\oint dk_x \mathcal{A}_x^{(n)}\right) = \frac{1}{e}\oint dk_y \partial_{k_y} P_1(k_y). \end{aligned}$$

Remarkably, in 4D there is a connection between a 4D generalization of the IQHE and a *magnetoelectric polarizability*, which plays an important part in the band theory approach to the 3D QSH state. We will discuss this later in Sec. 2.4.

1.3.2 The gradient expansion approach

In this subsection we use the gradient expansion to obtain the quantized Hall conductance. This is the first time we use this method to calculate a topological invariant. The idea and practical matters of the gradient expansion method are thoroughly explained in the Appendix C. The results of this subsection were first obtained by Volovik in 1988 [19].

So far, the discussion has been BT-oriented. The gradient expansion is a tool for deriving effective actions, and thus it is natural to start from the FT standpoint. The low-energy effective action of the IQH system is [52],

$$S_{QH} = \frac{\sigma_{xy}}{2}\int d^2\mathbf{x}dt\varepsilon^{\alpha\beta\gamma}\partial_\alpha A_\beta A_\gamma. \tag{1.12}$$

In a Landau-Ginzburg fashion, the action (1.12) can be taken as an ansatz built to satisfy our requirements. It is seen that the action breaks TRS since $(A_0, \mathbf{A}) \to (A_0, -\mathbf{A})$ under TR. Also Eq. (1.12) is the most relevant possible action in the renormalization group sense since it is lowest order in A. Most importantly, it gives the correct linear response,

$$j^i \equiv \frac{\delta S_{QH}}{\delta A_i} = \sigma_{xy}\varepsilon^{ji}\left(\partial_0 A_j - \partial_j A_0\right) = \sigma_{xy}\varepsilon^{ij}E_j,\ i,j=1,2. \tag{1.13}$$

In the gradient expansion approach we write the current differently. We can obtain the current from the path integral by integrating out the fermions (Appendix B),

$$j^\gamma = i\frac{\delta}{\delta A_\gamma}\text{Tr}\,\ln G = ie\int\frac{d^2\mathbf{k}d\omega}{(2\pi)^3}\text{tr}\,(G^{-1})_W\partial_{k_\gamma}\mathcal{G}. \tag{1.14}$$

Comparison to Eq. (1.13) shows that we have to expand $(G^{-1})_W$ to first order in the gradients of A. The lowest order term in the expansion is

$$(G^{-1})_{F,0} = e\frac{i}{2}F_{\alpha\beta}\mathcal{G}_0^{-1}\partial_{k_\alpha}\mathcal{G}_0\partial_{k_\beta}\mathcal{G}_0^{-1}$$

as is calculated in the Appendix C. Substitution to Eq. (1.14) yields

$$j^\gamma = -\frac{e^2}{2}\int\frac{d^2\mathbf{k}d\omega}{(2\pi)^3}F_{\alpha\beta}\mathrm{tr}\,\Lambda_{k_\gamma}\Lambda_{k_\alpha}\Lambda_{k_\beta},\ \Lambda_\alpha \equiv \mathcal{G}_0\partial_\alpha\mathcal{G}_0^{-1},$$

which can be integrated to obtain the QH action,

$$\begin{aligned}
S_{QH} =& -\frac{e^2}{4}\int d^2\mathbf{x}dt\int\frac{d^2\mathbf{k}d\omega}{(2\pi)^3}A_\gamma F_{\alpha\beta}\mathrm{tr}\,\Lambda_{k_\gamma}\Lambda_{k_\alpha}\Lambda_{k_\beta}\\
=& -\frac{e^2}{2}\int d^2\mathbf{x}dt\partial_{[\alpha}A_\beta A_{\gamma]}\int\frac{d^2\mathbf{k}d\omega}{(2\pi)^3}\mathrm{tr}\,\Lambda_{k_\gamma}\Lambda_{k_\alpha}\Lambda_{k_\beta}\\
=&\frac{\theta}{2}\int d^2\mathbf{x}dt\varepsilon^{\alpha\beta\gamma}\partial_\alpha A_\beta A_\gamma,\\
\theta =& -\frac{e^2}{2}\int\frac{d^2\mathbf{k}d\omega}{(2\pi)^3}\mathrm{tr}\,\Lambda_\omega\left(\Lambda_{k_x}\Lambda_{k_y}-\Lambda_{k_y}\Lambda_{k_x}\right).
\end{aligned}\tag{1.15}$$

Comparing to Eq. (1.12), we obtain the Hall conductance as a topological invariant,

$$\sigma_{xy} = \theta = -\frac{e^2}{2}\int\frac{d^2\mathbf{k}d\omega}{(2\pi)^3}\mathrm{tr}\,\varepsilon^{ij}\Lambda_\omega\Lambda_{k_i}\Lambda_{k_j}.$$

Calculation of the frequency integral shows this explicitly. Using the eigenvalue decom-

position of Appendix B, we have

$$\begin{aligned}
\int \frac{d\omega}{2\pi} \mathrm{tr}\, \varepsilon^{ij} \Lambda_\omega \Lambda_{k_i} \Lambda_{k_j} &= \int \frac{d\omega}{2\pi} \varepsilon^{ij} \sum_l \langle l| \Lambda_\omega \Lambda_{k_i} \Lambda_{k_j} |l\rangle \\
&= i \int \frac{d\omega}{2\pi} \varepsilon^{ij} \sum_{l,m,n,p} \langle l| \frac{|m\rangle\langle m|}{i\omega - E_m} \frac{|n\rangle\langle n|}{i\omega - E_n} \partial_{k_i} \mathcal{H}_0 \frac{|p\rangle\langle p|}{i\omega - E_p} \partial_{k_j} \mathcal{H}_0 |l\rangle \\
&= i \int \frac{d\omega}{2\pi} \varepsilon^{ij} \sum_{m,n} \frac{\langle n|\partial_{k_i} \mathcal{H}_0|m\rangle\langle m|\partial_{k_j} \mathcal{H}_0|n\rangle}{(i\omega - E_n)^2 (i\omega - E_m)} \\
&\overset{*}{=} i\varepsilon^{ij} \begin{cases} \sum_{m,n} \dfrac{\langle n|\partial_{k_i} \mathcal{H}_0|m\rangle\langle m|\partial_{k_j} \mathcal{H}_0|n\rangle}{(E_n - E_m)^2}, & E_n > E_F > E_m \\ -\sum_{m,n} \dfrac{\langle n|\partial_{k_i} \mathcal{H}_0|m\rangle\langle m|\partial_{k_j} \mathcal{H}_0|n\rangle}{(E_n - E_m)^2}, & E_m > E_F > E_n \end{cases} \\
&= -2i\varepsilon^{ij} \sum_{n \in \text{occ.}} \sum_{m \in \text{unocc.}} \frac{(\partial_{k_i} \mathcal{H}_\mathbf{k})_{nm} (\partial_{k_j} \mathcal{H}_\mathbf{k})_{mn}}{(E_n - E_m)^2}
\end{aligned}$$

yielding Eq. (1.10):

$$\sigma_{xy} = \frac{e^2}{h} i \int \frac{d^2\mathbf{k}}{2\pi} \varepsilon^{ij} \sum_{n \in \text{occ.}} \sum_{m \in \text{unocc.}} \frac{(\partial_{k_i} \mathcal{H}_\mathbf{k})_{nm} (\partial_{k_j} \mathcal{H}_\mathbf{k})_{mn}}{(E_n - E_m)^2}.$$

In the starred equality we employed the pole structure: The function

$$f(\omega) = (i\omega - E_n)^{-2} (i\omega - E_m)^{-1}$$

has residues $i(E_n - E_m)^{-2}$ at $-iE_n$, and $-i(E_n - E_m)^{-2}$ at $-iE_m$. The sum of these residues can only be finite if there is exactly one pole above the real axis.

We have shown that the correct topological invariant is obtained with the gradient expansion. The Green function integral (1.15) shows explicitly the topological nature of the Hall conductance. A small variation in the Green function is seen to induce no first order change in the conductivity, we will not show the calculation as it can be found in Ref. [5]. The robustness against small deformations of the Hamiltonian is yet another reason to call the transverse conductivity a topological invariant.

Chapter 2

Classification and dimensional reduction

In the previous chapter we encountered two physical systems showing nontrivial topologically protected phases. These phases could be labeled with a topological invariant which was either $\mathbb{Z}$- or $\mathbb{Z}_2$-valued. Furthermore, time-reversal symmetry and the spatial dimension had a fundamental role in how these phases manifest. Once it is known that there exists such interesting phases, one would like to find and classify all of them. Presumably the symmetries and spatial dimension play a role in the classification.

The edge modes and their stability provide a classification strategy. As was discussed, the QSH insulator edge modes are stable against TRI impurities and thus non-magnetic impurities cannot localize the edge states. This is because the edge modes are topologically protected – the topological invariant changes on the boundaries and forces the insulating gap to vanish. We also saw that not all edge states are topologically protected. In the 3D QSH there are weak TI phases which support gapless edge modes but these modes are not stable against disorder.

Thus, when one is interested in classifying topological insulators, one can start from the boundaries and inspect the stability, i.e., the localization properties of the edge modes. In particular, one would like to classify all boundary states which evade Anderson localization. This is in part what Schnyder and collaborators did in 2008 [53]. An alternative method, which we will review in this chapter, is to describe the bulk properties of generic Hamiltonians [53]. Either way leads to classifying random Hamiltonians, or random matrices, which reflect dynamics in the presence of random impurities. This is the Altland-Zirnbauer (AZ) classification introduced in the next section.

The classification results in the so-called periodic table of topological insulators [54], which will be reviewed in Sec. 2.2. This table lists the topological phases of all AZ symmetry classes in all spatial dimensions. It has to be remembered that other kinds of classification schemes are possible, for example, inversion symmetry is not one of the AZ symmetries [54, 55].

In the last part of this chapter, Secs. 2.3 and 2.4, we will introduce the method of dimensional reduction to explain how low dimensional topological phases are constructed from higher dimensional "parents". We will also discuss how one such parent is obtained with the gradient expansion. This is the important 4D CS field theory which is the parent for 3D and 2D QSH states.

2.1 The ten Altland-Zirnbauer symmetry classes

In this section we introduce the AZ symmetry classification [56, 57]. Let us consider a gapped single-particle Hamiltonian on a finite lattice,

$$H = \sum_{m,n} \psi^\dagger_{\alpha m} \mathcal{H}^{\alpha\beta}_{mn} \psi_{\beta n}$$

where $\psi_{\alpha n}$ annihilates a fermion specified by quantum numbers α, n and n labels the lattice site. From now on, we drop the label α to simplify notation. The Hamiltonian is thus described by a finite, say an $N \times N$, invertible matrix which we denote by $\mathcal{H}$.

We want to classify all gapped phases which support gapless edge modes in the phase boundaries. In addition, these modes have to be robust to small arbitrary perturbations that respect the symmetries of the system. For example, the QSH edge modes are robust to strong TRS disorder but become gapped in the presence of TRS breaking impurities. Therefore we want to investigate random gapped Hamiltonians according to their symmetries. In classifying these kind of Hamiltonians we cannot rely on unitary symmetries (described by unitary operators which commute with the Hamiltonian) as they would allow block decomposition of the Hamiltonian whereas we want to look at irreducible Hamiltonians. In the AZ classification the Hamiltonians are classified according to three fundamental discrete symmetries. The first is anticommutativity with a unitary matrix (chiral or sublattice symmetry). The remaining two are the time-reversal and charge conjugation (or particle-hole) symmetries (PHS), which are represented by antiunitary operations $\mathcal{T}$ and $\mathcal{C}$, respectively. These names often reflect the physical nature of the

symmetries. The three symmetries impose the following conditions on the Hamiltonian,

$$\text{Sublattice: } U_{\mathcal{S}}^{\dagger}\mathcal{H}U_{\mathcal{S}} = -\mathcal{H},\ U_{\mathcal{S}}^{2} = 1 \tag{2.1}$$

$$\text{Time-reversal: } U_{\mathcal{T}}^{\dagger}\mathcal{H}^{*}U_{\mathcal{T}} = \mathcal{H},\ \mathcal{T} = U_{\mathcal{T}}K,\ \mathcal{T}^{2} = \pm 1 \tag{2.2}$$

$$\text{Charge conjugation: } U_{\mathcal{C}}^{\dagger}\mathcal{H}^{*}U_{\mathcal{C}} = -\mathcal{H},\ \mathcal{C} = U_{\mathcal{C}}K,\ \mathcal{C}^{2} = \pm 1, \tag{2.3}$$

where K denotes complex conjugation. The matrices $U_{\mathcal{S}}, U_{\mathcal{T}}, U_{\mathcal{C}}$ are $N \times N$ unitary matrices which we refer to as "generators". If the Hamiltonian possesses any two of the above symmetries, it will also have the third which is given by either $U_{\mathcal{S}} = U_{\mathcal{T}}U_{\mathcal{C}}^{*}$ or $U_{\mathcal{T}/\mathcal{C}} = U_{\mathcal{S}}U_{\mathcal{C}/\mathcal{T}}$. The Hamiltonian can have the chiral symmetry even if it does not have the symmetries $\mathcal{T}$ and $\mathcal{C}$. Thus, whether we have an anti-unitary symmetry squaring to $+1$ or -1, or do not have that symmetry, we have in all 10 symmetry classes of Hamiltonians. These classes impose constraints on the corresponding space of time-evolution operators $\exp i\mathcal{H}t$. The ten spaces are actually the ten symmetric spaces of Cartan, which is the result first obtained by Zirnbauer and Altland [56, 57] in 1997. The ten symmetry classes are shown in the Table 2.1. Instead of time-evolution operators, we will be classifying so-called Q matrices which are introduced in the next section.

Before we introduce the Q matrix, it is instructive to go to momentum representation. Let us consider a periodic lattice system. In this case the Hamiltonian can be written in momentum space as $H = \sum_{\mathbf{k}} \psi_{\mathbf{k}}^{\dagger}\mathcal{H}_{\mathbf{k}}\psi_{\mathbf{k}}$ where the momentum vector $\mathbf{k} \in BZ$. The symmetry conditions (2.1, 2.2, 2.3) then relate the $N \times N$ matrix $\mathcal{H}_{\mathbf{k}}$ to $\mathcal{H}_{-\mathbf{k}}^{*}$. These conditions are directly obtained for momentum space Hamiltonians by replacing $\mathcal{H} \to \mathcal{H}_{\mathbf{k}}$ and $\mathcal{H}^{*} \to \mathcal{H}_{-\mathbf{k}}^{*}$ since the Fourier transform flips momentum on complex conjugation. The conditions (2.1, 2.2, 2.3) in momentum space with the gap condition $\det \mathcal{H} \neq 0$ allow us to draw some general conclusions about the energy spectra.

For the TRI Hamiltonians we have Kramers' degeneracy in the so-called time-reversal invariant momenta. The TRI momenta are the points in the BZ for which $k_i = -k_i \bmod 2\pi$ for all $i = 1, \ldots, d$. In these Kramers' degeneracy points if $|u_i(\mathbf{k})\rangle$ is an eigenstate of $\mathcal{H}_{\mathbf{k}}$ with an eigenvalue $E_i(\mathbf{k})$, then also $U_{\mathcal{T}}^{\dagger}|u_i(\mathbf{k})\rangle$ is an eigenstate with the same eigenvalue and$E_i(\mathbf{k})$ is doubly degenerate. As a corollary, the dimension of $\mathcal{H}_{\mathbf{k}}$, N is even.

Likewise, the sublattice symmetry dictates that N has to be even which is seen by taking the determinant in Eq. (2.1). The same holds for PHS insulators. For the chiral Hamiltonians the eigenvalues come in pairs because if $E_i(\mathbf{k})$ is an eigenvalue given by the state $|u_i(\mathbf{k})\rangle$, then $U_{\mathcal{S}}^{\dagger}|u_i(\mathbf{k})\rangle$ gives the eigenvalue $-E_i(\mathbf{k})$. A weaker result similar to Kramers' degeneracy holds for the PHS insulators: $E_i(\mathbf{k})$ and $-E_i(\mathbf{k})$ are both eigenvalues

but only for TRI momenta.

2.1.0.1 An example of the classification

To illustrate the classification scheme, we give some examples of the the four-band Hamiltonian

$$\mathcal{H}(\mathbf{k}) = \gamma_\mu d_\mu(\mathbf{k}) + \gamma_5 d_5(\mathbf{k}),\ \mu = 0, 1, 2, 3. \tag{2.4}$$

We will encounter Hamiltonians like this in Chapter 3. The parity of the components (d_μ, d_5) plays a crucial role in the classification. Let us choose the following representation for the 4×4 Euclidean Dirac matrices: $\gamma_0 = \tau_1, \gamma_i = \sigma_i\tau_3, \gamma_5 = \tau_2$. Since the Dirac matrices are hermitian, (d_μ, d_5) are real. Because of the anticommutativity, Eq. (2.4) is clearly chirally symmetric when any of d_μ, d_5 is missing. To inspect the TR and PH symmetries, we look at

$$\mathcal{H}^*(-\mathbf{k}) = \tau_1 d_0(-\mathbf{k}) + \sigma_1\tau_3 d_1(-\mathbf{k}) - \sigma_2\tau_3 d_2(-\mathbf{k}) + \sigma_3\tau_3 d_3(-\mathbf{k}) - \tau_2 d_5(-\mathbf{k}).$$

Often d_0 and d_5 are mass terms or similar and are even in $\mathbf{k}$, whereas $d_i\, i = 1, 2, 3$ are odd. This includes the models discussed in Chapter 3. With the above conditions, we have the PH symmetry

$$U_\mathcal{C}\mathcal{H}^*(-\mathbf{k})U_\mathcal{C}^{-1} = -\mathcal{H}(\mathbf{k}),\ U_\mathcal{C} = \sigma_1\sigma_3\tau_2,\ \mathcal{C}^2 = 1.$$

There is no 4×4 Dirac matrix that would anticommute with all the five present in (2.4). Chiral symmetry is thus prevented and we can conclude that there is no TRS either. Therefore the Hamiltonian belongs to the AZ class D.

If we set $d_5 = 0$ we obtain two new symmetries generated by $U_\mathcal{S} = \tau_2$ and $U_\mathcal{T} = \sigma_1\sigma_3$. Since $\mathcal{T}^2 = -1$, the symmetry class is DIII.

2.2 Q matrix and the periodic table

To extend the classification to topological phases we introduce the Q matrix. This matrix is formed from the Hamiltonian and contains all the topologically relevant information of the corresponding system, in a sense it divides the space of all Hamiltonians into topological equivalence classes.

Let us consider the periodic lattice Hamiltonian $H = \sum_\mathbf{k} \psi_\mathbf{k}^\dagger \mathcal{H}_\mathbf{k} \psi_\mathbf{k}$ introduced in the

end of Sec. 2.1. The band structure of the system is obtained by solving for each $\mathbf{k}$ the eigenvalue equation $\mathcal{H}_{\mathbf{k}}|u_i(\mathbf{k})\rangle = E_i(\mathbf{k})|u_i(\mathbf{k})\rangle$, where $i = 1, 2, \ldots, N$ labels the bands and the states $|u_i(\mathbf{k})\rangle$ are orthonormal. Because we have set the Fermi energy to zero, $E_F = 0$, all the eigenvalues are non-vanishing. Furthermore, we divide the bands to N_- negative energy bands (valence bands) and N_+ positive energy bands (conductance bands). We can smoothly transform our Hamiltonian into a so-called flat band Hamiltonian Q without crossing the Fermi level or closing the gap. In the Q matrix all the valence band states have an energy -1 and all the conductance band states have an energy $+1$. Moreover, the Q matrix has the same eigenstates as the original Hamiltonian and the two are topologically equivalent.

We can build the Q matrix explicitly in the following way. Let us first denote the valence band projector as $P_-(\mathbf{k}) \equiv \sum_{i=1}^{N_-} |u_i(\mathbf{k})\rangle\langle u_i(\mathbf{k})|$. The Q matrix is then defined as

$$Q(\mathbf{k}) \equiv 1 - 2P_-(\mathbf{k}) = \sum_{i}^{N} \epsilon_i |u_i(\mathbf{k})\rangle\langle u_i(\mathbf{k})|,$$

where $\epsilon_i = -1$ $(+1)$ for valence (conductance) band states. The last equality can be seen substituting the resolution of unity $1 = \sum_i |u_i(\mathbf{k})\rangle\langle u_i(\mathbf{k})|$. The last form shows that this is really the flat band Hamiltonian we wanted. Summing the energy eigenvalues gives the trace $\operatorname{tr} Q = N_+ - N_-$. Another important property of the hermitian Q is unitarity, $Q^2 = 1$. This follows directly from $\epsilon_i^2 = 1$ for all i.

There is a degeneracy in Q: we can rotate the valence and conductance band states unitarily among themselves, and therefore we should in fact consider representatives of equivalence classes, $[Q] \in U(N_- + N_+)/U(N_-) \times U(N_+)$, not all the elements of $U(N)$. If there are additional symmetry conditions (Eqs. (2.1), (2.2) or (2.3)) imposed on the Hamiltonian they will determine the space of allowed Q matrices. This space is called the *classifying space*. These spaces for the ten AZ classes are given in Table 2.1.

The symmetries of the system are characterized by the topology of the classifying space. The Q matrix defines a mapping $\mathbf{k} \mapsto Q(\mathbf{k})$ from the d-dimensional BZ to the classifying space and these mappings can in principle be classified with homotopy groups[1] [44]. These homotopy groups describe how many topological phases in d spatial dimensions there are for a given Hamiltonian (symmetry class). A list of the homotopy groups for all symmetry classes in all spatial dimensions d constitutes the periodic table

[1]Homotopy groups classify mappings from n-spheres S^n to a target space. The BZ is often not an n-sphere and therefore special means have to be taken before homotopy groups can be employed [54].

Cartan nomenclature	TRS	PHS	SLS	Classifying space	Non-trivial topological phase
A	0	0	0	$\frac{U(N_- + N_+)}{U(N_-) \times U(N_+)}$	IQH
AI	+1	0	0	$\frac{O(N_- + N_+)}{O(N_-) \times O(N_+)}$	
AII	-1	0	0	$\frac{Sp(N_- + N_+)}{Sp(N_-) \times Sp(N_+)}$	QSH
AIII	0	0	1	$U(N)$	
BDI	+1	+1	1	$O(N)$	
CII	-1	-1	1	$Sp(N)$	
D	0	+1	0	$O(2N)/U(N)$	
C	0	-1	0	$Sp(2N)/U(N)$	
DIII	-1	+1	1	$U(2N)/Sp(2N)$	^{3}He-B
CI	+1	-1	1	$U(N)/O(N)$	

Table 2.1: The ten Cartan symmetric spaces which classify the gapped single-particle Hamiltonians. Columns 2 to 4 are read as follows: 0 means no symmetry (meaning that the corresponding condition 2.1, 2.2 or 2.3 does not hold) while ± 1 means symmetry with the symmetry operation $\mathcal{T}$ or $\mathcal{C}$) squaring to ± 1. The last column gives the AZ class of experimentally realized non-trivial topological phases. For example, the IQH state requires no symmetries while the QSH state requires $\mathcal{T}$ and describes spin-1/2 particles. The last four classes from D to CI describe the so-called Bogoliubov-de Gennes superconducting systems.

of topological insulators and superconductors. It suffices to list only the dimensions from $d = 0$ to $d = 7$ because of a periodicity of 8 in the dimension.

Our homotopy argument is one way to understand the periodic table. In practice, Schnyder, Ryu, Furusaki and Ludwig did not do this, but instead constructed boundary modes for different symmetry classes and inspected which of the modes evade Anderson localization [53].

The periodic table is an important tool in the hunt for new topological phases. It does not only tell if a given material can have non-trivial topological phases, but it also gives hint of the so-called dimensional reduction procedure which we will discuss in Sec. 2.3. The periodic table is shown in Table 2.2.

Cartan nomenclature	$d=0$	$d=1$	$d=2$	$d=3$	$d=4$	$d=5$	$d=6$	$d=7$
A	$\mathbb{Z}$	-	$\mathbb{Z}$	-	$\mathbb{Z}$	-	$\mathbb{Z}$	-
AIII	-	$\mathbb{Z}$	-	$\mathbb{Z}$	-	$\mathbb{Z}$	-	$\mathbb{Z}$
AI	$\mathbb{Z}$	-	-	-	$2\mathbb{Z}$	-	$\mathbb{Z}_2$	$\mathbb{Z}_2$
BDI	$\mathbb{Z}_2$	$\mathbb{Z}$	-	-	-	$2\mathbb{Z}$	-	$\mathbb{Z}_2$
D	$\mathbb{Z}_2$	$\mathbb{Z}_2$	$\mathbb{Z}$	-	-	-	$2\mathbb{Z}$	-
DIII	-	$\mathbb{Z}_2$	$\mathbb{Z}_2$	$\mathbb{Z}$	-	-	-	$2\mathbb{Z}$
AII	$2\mathbb{Z}$	-	$\mathbb{Z}_2$	$\mathbb{Z}_2$	$\mathbb{Z}$	-	-	-
CII	-	$2\mathbb{Z}$	-	$\mathbb{Z}_2$	$\mathbb{Z}_2$	$\mathbb{Z}$	-	-
C	-	-	$2\mathbb{Z}$	-	$\mathbb{Z}_2$	$\mathbb{Z}_2$	$\mathbb{Z}$	-
CI	-	-	-	$2\mathbb{Z}$	-	$\mathbb{Z}_2$	$\mathbb{Z}_2$	$\mathbb{Z}$

Table 2.2: The periodic table of topological insulators and superconductors. The classes A and AIII form a separate block. The class A in 2D is has a $\mathbb{Z}$ invariant, this is the IQH state. Class AII in $d=2,3$ corresponds to the QSH state.

2.2.1 Block off-diagonal Q in chiral classes

A powerful result is that any chirally symmetric Q matrix can be written in the off-diagonal form

$$Q=\begin{pmatrix} 0 & q \\ q^\dagger & 0 \end{pmatrix},\ q\in U(N/2). \tag{2.5}$$

This has important consequences for chirally symmetric Hamiltonians, see Sec. 2.2.3.

Let us show the above property. The proof is elegant but not very useful since it does not explicitly give the basis transformation which leads to the Eq. (2.5). Let Q be the flat band matrix for a chirally symmetric Hamiltonian. Because of chirality, the Q matrix anticommutes with a unitary matrix $U_{\mathcal{S}}$: $QU_{\mathcal{S}}=-U_{\mathcal{S}}Q$. In Sec. 2.1 we saw that the eigenvalues of Q are paired meaning that $N_-=N_+$. In the basis where Q is diagonal we thus have $Q=\sigma_3\otimes 1$. The chiral generator in this basis can be written as

$$U_{\mathcal{S}}=\begin{pmatrix} 0 & u_{\mathcal{S}} \\ u_{\mathcal{S}}^\dagger & 0 \end{pmatrix},\ u_{\mathcal{S}}\in U(N/2).$$

There is a duality between the matrices Q and $U_{\mathcal{S}}$. This is because of the requirement $U_{\mathcal{S}}^2=1$ which makes $U_{\mathcal{S}}$ hermitian and have exactly the same properties as Q. In particular, its eigenvalues come in pairs and are ± 1. Therefore $U_{\mathcal{S}}$ can be diagonalized

to the form $U_{\mathcal{S}} = \sigma_3 \otimes 1$. This diagonalization brings Q to the block off-diagonal form we seek.

2.2.2 The classifying space of the classes A, AI, AII and AIII

To make the previous section more concrete, we construct the classifying space for the PHS breaking insulators, that is to say for the classes A, AI, AII, AIII. Because of the periodicity and certain shift properties of Table 2.2, it suffices to obtain the classification space in zero spatial dimensions. This corresponds to setting $\mathbf{k} \to 0$ in the conditions (2.1), (2.2) or (2.3) for the matrix $Q(\mathbf{k})$. This significantly simplifies the problem because otherwise we would have to relate $Q(\mathbf{k})$ to $Q(-\mathbf{k})$ in the antiunitary conditions. In this subsection we thus adopt the notation $Q \equiv Q(\mathbf{k} = 0)$.

2.2.2.1 A

We already deduced that $U(N_- + N_+)/U(N_-) \times U(N_+)$ is the classifying space for class A. Let us nevertheless make our reasoning a bit more precise. For the Q matrices we have the equivalence relation $\sim$ defined through $Q_1 \sim Q_2$ if $Q_1 = UQ_2U^\dagger$ for any $U \in U(N_-) \times U(N_+)$. The classifying space is the space of all inequivalent Q matrices, that is $U(N)/\sim = U(N_- + N_+)/U(N_-) \times U(N_+)$.

2.2.2.2 AI and AII

The classes AI and AII have the additional condition (2.2): $U_{\mathcal{T}}^\dagger Q^T U_{\mathcal{T}} = Q$ where $U_{\mathcal{T}} = U_{\mathcal{T}}^T$ for AI and $U_{\mathcal{T}} = -U_{\mathcal{T}}^T$ for AII.

In case of AI, the symmetric unitary matrix$U_{\mathcal{T}}$ can be written as $U_{\mathcal{T}} = UU^T$ where U is unitary [58]. Transforming to a basis $|u_i\rangle \to U^*|u_i\rangle$ gives $Q \to U^*QU^T$ and the condition (2.2) in the new basis reads $U^*U^\dagger \left(U^*QU^T\right)^T UU^T = U^*QU^T$ or $Q^T = Q$. Thus $Q \in O(N)$. We have still a freedom to transform the states with real orthogonal matrices. As in the case of A, the classifying space is thus $O(N_- + N_+)/O(N_-) \times O(N_+)$.

For AII we have the condition $Q^T U_{\mathcal{T}} Q = U_{\mathcal{T}}$ with $U_{\mathcal{T}}$ antisymmetric. The antisymmetric unitary matrix $U_{\mathcal{T}}$ can be written in block matrix form

$$D = \begin{pmatrix} 0 & 1_{N/2} \\ -1_{N/2} & 0 \end{pmatrix} = R^T U_{\mathcal{T}} R$$

with a real orthogonal matrix R. Consequently, transforming to a basis $|u_i\rangle \to R|u_i\rangle$

which gives $Q \to RQR^T$, the condition (2.2) reads $RQ^TR^TU_{\mathcal{T}}RQR^T = U_{\mathcal{T}}$ or $Q^TDQ = D$. This defines the space of symplectic matrices $Sp(N)$ and $Q \in Sp(N)$. We have still a freedom to transform the states as $|u_i\rangle \to B|u_i\rangle$ where B is now a symplectic matrix, $B^TDB = D$. Thus the classifying space for AII is $Sp(N_- + N_+)/Sp(N_-) \times Sp(N_+)$.

2.2.2.3 AIII

In this case we have only the chiral symmetry. Writing the Q matrix in the block off-diagonal form of Eq. (2.5) gives the only constraint: the off-diagonal component q has to belong to $U(N/2)$. Therefore the classifying space for class AIII is $U(N/2)$.

2.2.3 Winding number for chiral insulators in odd spatial dimensions

In this subsection, we discuss the topological invariant for chirally symmetric systems. This topological invariant is given by a simple-looking winding number ν written in terms of the Q-matrix of the system [53, 54]. We give an equivalent formula for this winding number. As seen from table 2.2, AIII insulators are classified by an integer invariant in odd spatial dimensions. The same winding number applies to classes CI, CII, DIII and BDI but all integers may not be obtained depending on space dimension and symmetry class. For example, for class CI in $d = 3$ the winding number ν is even.

Let the block off-diagonalized Q-matrix for a chiral insulator be

$$Q_{\mathbf{k}} = \begin{pmatrix} 0 & q_{\mathbf{k}} \\ q_{\mathbf{k}}^\dagger & 0 \end{pmatrix},$$

the corresponding winding number is given by the integral [54]

$$\nu_{2n+1} = \int_{BZ} d^{2n+1}\mathbf{k}(-1)^n n! \left(\frac{i}{2\pi}\right)^{n+1} \mathrm{tr}\,(q_{\mathbf{k}}^{-1}\partial_{[k_{\alpha_1}} q_{\mathbf{k}}) \dots (q_{\mathbf{k}}^{-1}\partial_{k_{\alpha_{2n+1}}]} q_{\mathbf{k}}). \tag{2.6}$$

In particular, this equation gives an explicit expression for the topological invariant of AIII insulators, and therefore is quantized to integers. Equation (2.6) also seems like a convenient calculational tool for classifying any given chirally symmetric Hamiltonian. There is a catch however. Namely, to be able to write down the Q-matrix, one needs to calculate the projector, which in turn is equivalent to diagonalizing the Hamiltonian. After this one off-diagonalizes the Q-matrix and gets a complicated expression for $q_{\mathbf{k}}$.

With a realistic lattice model the integral of Eq. (2.6) is extremely tedious to evaluate even numerically. For a Dirac Hamiltonian, i.e., linearized spectrum, the matrix q is often not too complicated and Eq. (2.6) can be calculated (usually numerically). To tackle these problems, we introduce a more convenient way to evaluate the invariant ν. We will do this specifically in 3D ($n = 1$) where it is of most practical use. A generalization to any odd spatial dimension is straightforward.

To start, we introduce a new topological invariant, N^K. For any Hamiltonian $\mathcal{H}$, it is given by the 3-form integral [59]

$$N^K = \frac{1}{4\pi^2} \int d^3\mathbf{k} \, \mathrm{tr}\, K\mathcal{H}^{-1}\partial_{[k_x}\mathcal{H}\mathcal{H}^{-1}\partial_{k_y}\mathcal{H}\mathcal{H}^{-1}\partial_{k_z]}\mathcal{H}, \tag{2.7}$$

where K anticommutes with $\mathcal{H}$. N^K is a topological invariant[2] written in terms of the zero-frequency Green functions $\mathcal{H}^{-1} \equiv \mathcal{G}(\mathbf{k}, \omega = 0)$. This invariant is naturally generalizable to any odd spatial dimensions. It might seem strange that it is written in terms of the Hamiltonian, not the Green function. This can be understood heuristically: In odd spatial dimensions, if one tries to write a Green function invariant one needs an even number of 1-forms $\mathcal{G}d\mathcal{G}^{-1}$, since the space-time dimension is even. But now since we have an antisymmetric combination, the trace always vanishes trivially.

We will show that the invariant ν_3 is proportional to N^K:

$$\nu_3 = -\,2N^K. \tag{2.8}$$

Now we proceed to derive Eq. (2.8). Let $\mathcal{H}(\mathbf{k})$ be a $2N$-dimensional chirally symmetric Hamiltonian written in momentum space. As shown in Sec. 2.2.1, we can choose a chiral generator $U_\mathcal{S} = \sigma_3 \otimes 1$ meaning that the Hamiltonian can be written in the block off-diagonal form

$$\mathcal{H} = \sigma_+ \otimes h + \sigma_- \otimes h^\dagger, \tag{2.9}$$

where h is an $N \times N$ matrix. Now we can actually make h unitary by flattening the bands, which does not change the topological class of the system. Let us denote the flat band Hamiltonian as $\mathcal{H}_F$, which is also unitary, $\mathcal{H}_F^{-1} = \mathcal{H}_F$. We substitute Eq. (2.9) into

[2]The topological invariance of N^K is seen by varying the Hamiltonian and observing no first order change in N^K. The calculation is exactly the same as with the Green function invariant in Subsec. 1.3.2.

Eq. (2.7). The trace over the Pauli matrices can be calculated

$$\begin{aligned} N^K =& \frac{1}{4\pi^2}\int d^3\mathbf{k}\,\mathrm{tr}\,K\mathcal{H}^{-1}\partial_{[k_x}\mathcal{H}\mathcal{H}^{-1}\partial_{k_y}\mathcal{H}\mathcal{H}^{-1}\partial_{k_z]}\mathcal{H} \\ =& \frac{1}{4\pi^2}\int d^3\mathbf{k}\,\mathrm{tr}\,\sigma_3 h_F^\dagger\sigma_-\partial_{[k_x}h_F\sigma_+h_F^\dagger\sigma_-\partial_{k_y}h_F\sigma_+h_F^\dagger\sigma_-\partial_{k_z]}h_F\sigma_+ \qquad (2.10) \\ &+\frac{1}{4\pi^2}\int d^3\mathbf{k}\,\mathrm{tr}\,\sigma_3 h_F\sigma_+\partial_{[k_x}h_F^\dagger\sigma_-h_F\sigma_+\partial_{k_y}h_F^\dagger\sigma_-h_F\sigma_+\partial_{k_z]}h_F^\dagger\sigma_- \\ =& \frac{-2}{4\pi^2}\int d^3\mathbf{k}\,\mathrm{tr}\,\frac{1}{h_F}\partial_{[k_x}h_F\frac{1}{h_F}\partial_{k_y}h_F\frac{1}{h_F}\partial_{k_z]}h_F = -2N^K, \qquad (2.11) \end{aligned}$$

since $h_F = q$. This is a useful and an important result because the invariant N^K in its basic form Eq. (2.7) is simple to calculate whereas Eq. (2.6) is exceptionally hard.

2.3 Dirac Hamiltonians and dimensional reduction

Despite its somewhat promising name, the periodic table 2.1 is not everything there is to topological phases. Within a symmetry class in a fixed spatial dimension there can be several topological states of matter that need to be found and distinguished. This can be done by identifying the correct topological invariant and then calculating the invariant for different systems, hoping to see diversity. This calculation of the topological invariants can be a tedious task as we have seen. However, topological invariance gives substantial aid in the search for yet undiscovered topological phases. Topology has the powerful property that it suffices to only consider a single representative of a phase and this representative depicts all the topological properties of the phase. In particular, if we know that a complicated system is adiabatically connected to a simple system, then it is enough to calculate the topological invariant only for the simple system.

The simple system we refer to is most often a massive d-dimensional Dirac model

$$\mathcal{H}_d(\mathbf{k}) = \Gamma_d^i k_i + \Gamma_d^0 m,\ i = 1, 2, \ldots, d \qquad (2.12)$$

where the $d+1$ matrices Γ_d^i obey the Clifford algebra $[\Gamma_d^i, \Gamma_d^j]_+ = 2\delta^{ij}$. There exists a Dirac representative for all the 10 AZ symmetry classes in all dimensions [54].

Any massive Dirac Hamiltonian $\mathcal{H}_d(\mathbf{k})$ can be constructed from a higher dimensional massless Dirac Hamiltonian

$$\mathcal{H}_{d+1}(\mathbf{k}) = \Gamma_{d+1}^i k_i,\ i = 1, 2, \ldots, d+1$$

through a process called dimensional reduction. The dimensional reduction is a compactification of the extra dimension in the spirit of Kaluza and Klein. A compactification of the $(d+1)$th dimension to a circle of radius R quantizes the $(d+1)$th momentum component to discrete values that scale like $1/R$. Making $R \to 0$ pushes any finite k_{d+1} to arbitrarily large energies and we can neglect them. In particular, $\mathcal{H}_{d+1}(\mathbf{k})$ looks like a d dimensional massless Hamiltonian with momentum $\mathbf{k} = (k_1, k_2, \ldots, k_d, 0)$.

We can obtain the massive Hamiltonian (2.12) through a fictitious external electromagnetic field $\mathbf{A}$. The field is minimally coupled to momentum, $\mathbf{k} \to \mathbf{k} + e\mathbf{A}$. Doing the dimensional reduction as before and then setting $A_\mu = \delta_{\mu,d+1} m$ gives the massive d dimensional Dirac model.

2.4 4D CS Effective Field Theory

An important EFT is the 4D CS theory introduced first by Zhang and Hu as a generalization of the QHE in 4D [49]. It was brought up in the context of topological insulators by Qi and co-workers [5]. This FT is given by the electromagnetic action

$$S = \frac{C_2 e^3}{24\pi^2} \int d^4\mathbf{x} dt \varepsilon^{\alpha\beta\gamma\delta\epsilon} \partial_\alpha A_\beta \partial_\gamma A_\delta A_\epsilon, \quad \alpha, \beta, \ldots = 0, \ldots, 4. \tag{2.13}$$

Analogous to the 2D CS action, also this model has a $\mathbb{Z}$ invariant which in this case is the second Chern number C_2 of Eq. (1.7). This number is obtained from the non-Abelian momentum space Berry connection

$$\mathcal{A}^{mn} = \langle m, \mathbf{k}| \, \partial_{k_i} \, |n, \mathbf{k}\rangle \, dk_i.$$

Contrary to its 2D twin, the action (2.13) is TRS. From the dimensional reduction to 3D and 2D one obtains a $\mathbb{Z}_2$ invariant which is the second Chern parity. This describes the QSH phases, or AII insulators, in 3D and 2D [5] and represents an instance of the $\mathbb{Z} \to \mathbb{Z}_2 \to \mathbb{Z}_2$ structure seen in the periodic table 2.2. In the next subsection, we give as an example the dimensional reduction to 3D.

2.4.1 Dimensional reduction to 3D

The 4D CS action (2.13) gives also the EFT of the lower dimensional TRS topological insulators [5]. Taking x_4 as the extra dimension and setting $\partial_4 A_\mu = 0$ for $\mu = 0, \ldots, 3$

yields the axion electrodynamics action [25]

$$S = \frac{e^2}{32\pi^2}\varepsilon^{\alpha\beta\gamma\delta}\int d^3\mathbf{x}dtF_{\alpha\beta}F_{\gamma\delta}\theta = \frac{e^2}{4\pi^2}\int d^3\mathbf{x}dt\mathbf{E}\cdot\mathbf{B}\theta, \quad \alpha,\beta,\ldots = 0,\ldots,3 \tag{2.14}$$

with an axion angle $\theta = eC_2\oint dx_4 A_4$. This action provides the basis for the magnetoelectric effect and will be discussed also in Chapter 3. The integral $\phi \equiv \oint dx_4 A_4$ is the flux threading the compactified fourth dimension. This flux is only defined modulo 2π because to physics a 2π change makes no difference[3]. TR symmetry poses an important contraint for the value of the flux: because TR takes ϕ to $-\phi$, the flux should be either 0 or $\pi = -\pi \bmod 2\pi$.

The axion angle defines a generalized, *magnetoelectric polarizability* $P_3 = \theta/2\pi$, which is the 3D equivalent of the 1D polarization P_1 we glanced at in Sec. 1.3. In a complete analogy, P_3 can be expressed as an integral

$$P_3 = \frac{e}{8\pi^2}\int d^3\mathbf{k}\sum_{n\in\text{occ}}\left(\mathcal{A}\wedge d\mathcal{A} + \frac{2}{3}\mathcal{A}\wedge\mathcal{A}\wedge\mathcal{A}\right)^{nn}$$

in close connection to the second Chern number and Eq. (1.5). The 3D integral is gauge invariant only modulo of an integer and thus P_3 has an integer ambiguity. When TRS is imposed, only values 0 and 1/2 are allowed for P_3 and if TRS is broken, P_3 can have any value in the interval $[0, 1]$. We shall next see that $P_3 = 1/2$ characterizes a TRI topological insulator.

Consider an interface between a trivial and a non-trivial 3D insulator. In the boundary, the magnetoelectric polarization P_3 changes from 0 to 1/2. If we break TRS on the surface, we will have an inhomogeneous P_3 which leads to a half-integer QHE on the surface of the 3D insulator. Let A be constant in the z-direction andP_3 vary, the current from Eq. (2.14) is then

$$j^\alpha = \frac{e^2}{h}\partial_z P_3\varepsilon^{\alpha\beta\gamma}\partial_\beta A_\gamma, \quad \alpha,\beta,\ldots = 0,\ldots,2$$

which is the QH response introduced in Subsec. 1.3.2. Integrating the current density j^α over the interface leads to a Hall conductance $\sigma_{xy} = \pm e^2/2h$ in the $x-y$ plane [5, 6, 4]. This half-integer QHE distinguishes the trivial and non-trivial insulating states and gives a $\mathbb{Z}_2$ classification.

[3]This is because of gauge invariance, for example, the electron wave function obtains a phase shift $e^{i\chi}$ in a gauge transformation $A_\mu \to A_\mu + \partial_\mu\chi,\ \mu = 0,\ldots,4$.

2.5 4D CS with the gradient expansion

In this section we show how the effective action of the 4D CS FT is obtained through the gradient expansion. The second Chern number C_2 of Eq. (2.13) can be expressed as a Green function integral similar to the first Chern number C_1 in the 2D CS theory (see Subsec. 1.3.2 and the remark in Chapter B). This was shown by Qi et al. [5]. Knowing this result it is enough to show that we obtain the same Green function integral.

The action we seek is Eq. (2.13) and proportional to the second power of the field tensor $F_{\alpha\beta}$. Therefore the term we extract from the gradient expansion (C.7) is $(G_0^{-1})_{FF,0}$. This term is given in the Section C.3 of the Appendix,

$$(G_0^{-1})_{FF,0} = -\frac{e^2}{4}F_{\alpha\beta}F_{\gamma\delta}\left[\mathcal{G}_0^{-1}\partial_{k_\delta}\mathcal{G}_0\partial_{k_\gamma}\left(\partial_{k_\beta}\mathcal{G}_0^{-1}\partial_{k_\alpha}\mathcal{G}_0\mathcal{G}_0^{-1}\right) + \frac{1}{2}\mathcal{G}_0^{-1}\partial_{k_\gamma}\left(\partial_{k_\beta}\mathcal{G}_0\partial_{k_\alpha}\partial_{k_\delta}\mathcal{G}_0^{-1}\right)\right].$$

To obtain the completely antisymmetric action (2.13) we drop the last term, which at least for Dirac Hamiltonians does not contribute. We start by expanding the current (B.2) of the generic effective action

$$j^\epsilon = \frac{\delta}{\delta A_\epsilon} i\mathrm{Tr}\,\ln G = ie\int\frac{d^3\mathbf{k}d\omega}{(2\pi)^4}\,\mathrm{tr}\,(G^{-1})_W\partial_{k_\epsilon}\mathcal{G}.$$

Substituting and collecting $(G_0^{-1})_{FF,0}$ we get

$$\begin{aligned} j^\epsilon =& -i\frac{e^3}{4}F_{\alpha\beta}F_{\gamma\delta}\int\frac{d^3\mathbf{k}d\omega}{(2\pi)^4}\,\mathrm{tr}\,\partial_{k_\epsilon}\mathcal{G}_0\partial_{k_\gamma}\mathcal{G}_0^{-1}\partial_{k_\delta}\mathcal{G}_0\partial_{k_\alpha}\mathcal{G}_0^{-1}\partial_{k_\beta}\mathcal{G}_0\mathcal{G}_0^{-1} \\ =& \frac{ie^3}{4}F_{\alpha\beta}F_{\gamma\delta}\int\frac{d^3\mathbf{k}d\omega}{(2\pi)^4}\,\mathrm{tr}\,\Lambda_{k_\alpha}\Lambda_{k_\beta}\Lambda_{k_\gamma}\Lambda_{k_\delta}\Lambda_{k_\epsilon}. \end{aligned}$$

Integrating over A_ϵ yields the action

$$\begin{aligned} S =& \frac{ie^3}{12}\int d^4\mathbf{x}dtF_{\alpha\beta}F_{\gamma\delta}A_\epsilon\int\frac{d^4\mathbf{k}d\omega}{(2\pi)^5}\,\mathrm{tr}\,\Lambda_{k_\alpha}\Lambda_{k_\beta}\Lambda_{k_\gamma}\Lambda_{k_\delta}\Lambda_{k_\epsilon} \\ =& i\frac{e^3}{3}\int d^4\mathbf{x}dt\partial_{[\alpha}A_\beta\partial_\gamma A_\delta A_{\epsilon]}\int\frac{d^4\mathbf{k}d\omega}{(2\pi)^5}\,\mathrm{tr}\,\Lambda_{k_\alpha}\Lambda_{k_\beta}\Lambda_{k_\gamma}\Lambda_{k_\delta}\Lambda_{k_\epsilon} \\ =& \frac{\theta e^3}{24\pi^2}\int d^4\mathbf{x}dt\varepsilon^{\alpha\beta\gamma\delta\epsilon}\partial_\alpha A_\beta\partial_\gamma A_\delta A_\epsilon, \\ \theta =& \frac{i\pi^2}{15}\int\frac{d^4\mathbf{k}d\omega}{(2\pi)^5}\,\mathrm{tr}\,\varepsilon^{\alpha\beta\gamma\delta\epsilon}\Lambda_{k_\alpha}\Lambda_{k_\beta}\Lambda_{k_\gamma}\Lambda_{k_\delta}\Lambda_{k_\epsilon} \end{aligned}$$

The θ is the Green function integral obtained in Ref. [5] and is actually the second Chern number $\theta = C_2$. Thus we have obtained the 4D CS FT with the topological prefactor C_2.

Chapter 3

Solitons in topological media

In the previous chapters we have seen the gradient expansion in use. We have considered Wigner transformed Green functions where all the large scale spatial variation is in the 4-vector potential A. In this chapter we extend the discussion to Green functions which are inherently spatially slowly varying. We combine in a new way the momentum space topology discussed earlier with real space topology that fits into the Landau symmetry breaking paradigm.

The gradient expansion provides us a useful tool to investigate *topological solitons* in different physical systems. In condensed matter physics the topological objects of interest are usually *singular* defects such as domain walls (Fig. 3.1), vortices, dislocations or kinks [60]. Here the word singular means that the degeneracy parameter[1] is not well-defined everywhere. These objects are described by conventional homotopy groups, which classify mappings from a region of the medium to the space of the degeneracy parameter [11, 44], also called the *moduli space*. In this chapter we describe topological objects of different nature, i.e., *non-singular* objects. Non-singular or continuous topological structures are called topological solitons or textures and they have well-defined degeneracy parameters everywhere in the medium. Examples of textures are the Bloch and Néel domain walls in ferromagnets or the analogous mass domain wall in Fig. 3.2.

Just like defects, continuous topological textures can be classified topologically. This is because inside the soliton the symmetry group of the moduli space can be less restricted and some symmetries of the bulk can be broken. In other words, the moduli space can be extended inside the soliton. The topological classification is not acquired from homotopy

[1] In the systems we discuss the degeneracy parameter is the phase factor of the order parameter. For example in ferromagnets it is $\mathbf{m}/|\mathbf{m}|$ where $\mathbf{m}$ is the magnetization.

groups, but requires the notion of *relative homotopy groups* [61, 62]. In this context a relative homotopy group is defined for two moduli spaces, those corresponding to the interior P and the exterior $Q \subset P$ of the soliton. The relative homotopy group is denoted $\pi_d(P, Q)$ and it can be calculated from the exact sequence[2] [63]

$$\ldots \longrightarrow \pi_d(Q) \longrightarrow \pi_d(P) \longrightarrow \pi_d(P, Q) \longrightarrow \pi_{d-1}(Q) \longrightarrow \ldots \tag{3.1}$$

The results presented in this chapter are published in Ref. [64].

3.1 Mass domain walls in a 3D Dirac model

Let us start with a simple system which provides an example of both singular and non-singular domain walls. Consider the following massive TRS four-band Hamiltonian

$$H(\mathbf{k}) = \boldsymbol{\gamma} \cdot \mathbf{k} + \gamma_0 m, \tag{3.2}$$

which is chirally symmetric as it anticommutes with γ_5. Time-reversal and PH symmetries are generated by $\gamma_1\gamma_3$ and $\gamma_1\gamma_3\gamma_5$, respectively and the Hamiltonian belongs to the AZ class DIII, see Sec. 2.3. The system has a topological charge given by the momentum space integral [59]

$$N^K = \frac{1}{4\pi^2} \int d^3\mathbf{k} \, \mathrm{tr}\, \gamma_5 \mathcal{H}^{-1} \partial_{[k_x} \mathcal{H} \mathcal{H}^{-1} \partial_{k_y} \mathcal{H} \mathcal{H}^{-1} \partial_{k_z]} \mathcal{H},$$

already introduced in Section 2.2.3. For Eq. (3.2) the integral gives $N^K = \mathrm{sgn}\, m$ which is the degeneracy parameter of our system.

Consider now two regions in space (or the bulk), $z < 0$ and $z > 0$, corresponding to positive and negative mass m. In the language introduced in the beginning of this chapter, the boundary between the two regions is a singular domain wall or a kink [60]. The TR and chiral symmetries are obeyed everywhere. When the invariant N^K changes, necessarily the mass vanishes producing a gapless phase in the interface. Wherever the gap closes, the invariant N^K is not well-defined. One can define a parity n by the equation $(-1)^n = N^K(z < 0)N^K(z > 0)$, which is even if there is no domain wall.

Hamiltonian (3.2) also provides an example of a texture, or non-singular domain wall.

[2] An exact sequence $F \to G \to H$ is such that for any group homomorphism $f : F \to G$ the image of f is the kernel of the next homomorphism $g : G \to H$.

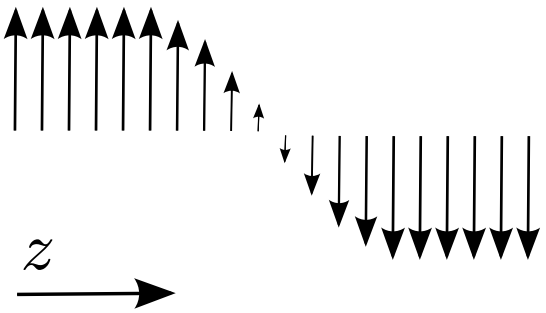

Figure 3.1: A singular mass domain wall. The arrows depict the order parameter field and the direction of the arrows is the degeneracy parameter N^K which is not defined everywhere.

In constructing a non-singular soliton we want to keep the system gapped *everywhere* and consequently we will add another mass term in the Hamiltonian (3.2). The region in space where this new mass component is non-zero defines the soliton or texture. To add the mass we have to break some symmetries, which we allow as was discussed in the beginning of this chapter. In particular, we allow the mass to be complex-valued[3] and hence extend the above moduli space $Q = \mathbb{Z}_2$ to the circle $P = S^1$.

We define a new Hamiltonian

$$H(\mathbf{k}, z) = \boldsymbol{\gamma} \cdot \mathbf{k} + \gamma_0 m_1(z) + \gamma_5 m_2(z) \tag{3.3}$$

where the mass is allowed to vary in the z-direction,

$$m_1(z) = \begin{cases} m, & z < 0 \\ m \cos z n\pi, & z \in [0,1] \\ (-1)^n m, & z > 1 \end{cases}$$

$$m_2(z) = \begin{cases} 0, & z \notin [0,1] \\ m \sin z n\pi, & z \in [0,1] \end{cases}$$

and the textured region is the "thick plane" $\mathbb{R} \times \mathbb{R} \times [0,1]$. The symmetries are preserved outside this region, and the Hamiltonian (3.2) is restored. For notational simplification we are using dimensionless lengths. We chose the mass m_2 so that the gap is constant within the soliton, $H^2 \equiv E^2 = \mathbf{k}^2 + m^2$ for all z. Of course any other choice for the m in

[3]This should not be taken too literally. The "complex plane" in this case is spanned by "vectors" γ_0 and γ_5, the latter corresponding to the imaginary unit.

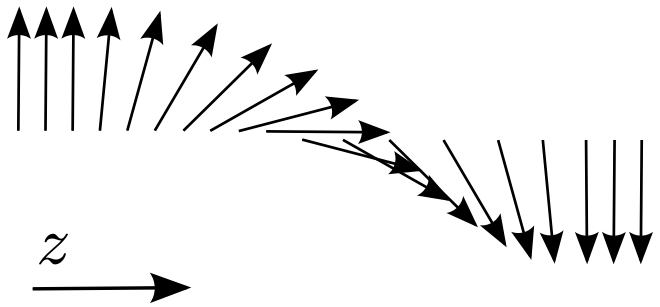

Figure 3.2: A non-singular mass domain wall with $n = 1$. The length of the vector is constant everywhere. The tilt of the vector depicts the angle $\pi n z$.

$m_2 = m \sin z n \pi$ would be equally good, the only requirement is that the gap $m_1^2 + m_2^2$ is finite everywhere.

In the case of the singular domain wall, the topological charge was determined by the homotopy group $\pi_0(\mathbb{Z}_2) = \mathbb{Z}_2$ or the parity n. As we discussed above, the invariant for the textured system is given by the relative homotopy group $\pi_1(S^1, \mathbb{Z}_2)$. In the end of this section we show that $\pi_1(S^1, \mathbb{Z}_2) = \mathbb{Z}_2 \times \mathbb{Z}$ reflecting the winding number inside the texture. The invariant of the non-singular system can be expressed by the Green function integral

$$N_5 = \frac{1}{4\pi^3 i} \int dz \int d^3k d\omega \, \mathrm{tr}\, \mathcal{G}\partial_{[k_x}\mathcal{G}^{-1}\mathcal{G}\partial_{k_y}\mathcal{G}^{-1}\mathcal{G}\partial_{k_z}\mathcal{G}^{-1}\mathcal{G}\partial_{\omega}\mathcal{G}^{-1}\mathcal{G}\partial_{z]}\mathcal{G}^{-1} \qquad (3.4)$$

where the z-integral is calculated over the texture $[0, 1]$ and the Green functions are in the Wigner representation,

$$\mathcal{G}(\mathbf{k}, \omega, z) = \frac{1}{i\omega - H} = -\frac{i\omega + H}{\omega^2 + E^2}.$$

For the linear Hamiltonian (3.3) the integral (3.4) can be calculated analytically and it is evaluated in Section B.1 of the Appendix B. The result is $N_5 = n/2$. This invariant N_5 contains information from both outside and inside of the texture and also embodies the relative homotopy group $\mathbb{Z}_2 \times \mathbb{Z}$ which is the group of half-integers. Inside, $\lfloor n/2 \rfloor$ counts how many times the complex mass $me^{i\pi nz}$ winds around the origin in the complex plane. Outside, the parity of n determines whether the states on the two sides of the interface belong to the same topological class.

Finally, to illustrate the relative homotopy group, let us show that $\pi_1(P, Q) = \mathbb{Z}_2 \times \mathbb{Z}$. Knowing $Q = \mathbb{Z}_2$ and $P = S^1$ we can calculate the homotopy groups $\pi_{0,1}(Q)$ and $\pi_{0,1}(P)$.

Substituting these into the exact sequence (3.1) yields

$$1 \longrightarrow \mathbb{Z} \longrightarrow \pi_1(P,Q) \longrightarrow \mathbb{Z}_2 \longrightarrow 1.$$

From this we get the following set of equations,

$$\begin{aligned} 1 = \text{Im } (1 \longrightarrow \mathbb{Z}) &= \text{Ker } (\mathbb{Z} \longrightarrow \pi_1(P,Q)) \\ \text{Im } (\mathbb{Z} \longrightarrow \pi_1(P,Q)) &= \text{Ker } (\pi_1(P,Q) \longrightarrow \mathbb{Z}_2) \\ \text{Im } (\pi_1(P,Q) \longrightarrow \mathbb{Z}_2) &= \text{Ker } (\mathbb{Z}_2 \longrightarrow 1) = \mathbb{Z}_2. \end{aligned}$$

Now recall that for any group homomorphism $f : F \to G$ we have $\text{Im}\, f = F/\text{Ker}\, f$. This means that

$$\mathbb{Z} = \text{Im } (\mathbb{Z} \longrightarrow \pi_1(P,Q)) = \text{Ker } (\pi_1(P,Q) \longrightarrow \mathbb{Z}_2)$$

giving $\mathbb{Z}_2 = \pi_1(P,Q)/\mathbb{Z}$, or $\pi_1(P,Q) = \mathbb{Z}_2 \times \mathbb{Z}$ – the group of half-integers.

3.2 Axion electrodynamics and the QHE

As another example of a texture, we consider the four-band lattice model for a TRI topological insulator introduced in Ref. [28]. The Hamiltonian is given by

$$H(\mathbf{k}) = -2\lambda(\gamma_1 \sin k_x + \gamma_2 \sin k_y + \gamma_3 \sin k_z) + \gamma_0 m_1(\mathbf{k}), \tag{3.5}$$

where $m_1(\mathbf{k}) = \epsilon - 2t(\cos k_x + \cos k_y + \cos k_z)$ and γ_μ are the 4×4 Dirac matrices. It was shown in Chapter 2 that this Hamiltonian belongs to the class DIII of topological insulators. It is claimed that this system exhibits a non-trivial topological phase with parameter values $2t < \epsilon < 6t$. In this phase the system serves as an axion medium, i.e., it should allow a finite axion angle θ in the action [28]

$$S_{FF} = \frac{e^2}{32\pi^2}\varepsilon^{\alpha\beta\gamma\delta} \int d^3\mathbf{x}dt F_{\alpha\beta}F_{\gamma\delta}\theta, \tag{3.6}$$

which we have seen before in Sec. (2.4). Because of TRI, the axion angle θ can take only two values, 0 and π, providing a $\mathbb{Z}_2$ classification of the system. We also saw in Sec. 2.4, that this action leads to a QHE in the $x-y$-plane between separating a TI and a trivial insulator. The Hall conductance was found to be $\sigma_{xy} = e^2 \int dz \partial_z \theta/2\pi h$ when we assumed that the vector potential A is independent of the z-coordinate and TRS is broken on the

surface.

It is not completely resolved if the Hamiltonian (3.5) has a $\mathbb{Z}$ or $\mathbb{Z}_2$ invariant – it belongs to AZ class DIII which has a $\mathbb{Z}$ invariant. This is related to whether the integer ambiguity of the polarizability P_3 can be observed or not. In Subsec. 3.2.1 below, we obtain results controversial to those stated above. We show that introducing a textured region in the bulk leads to a QHE on its surface, with *any* half-integer conductance. The soliton is characterized by a $\mathbb{Z}$ invariant. Moreover, we show that in fact the term (3.6) is absent in the action, but is replaced by a related term [65]

$$S_{AF} = \frac{e^2}{16\pi^2}\varepsilon^{\alpha\beta\gamma\delta}\int d^3\mathbf{x}dt F_{\alpha\beta}A_\gamma\nabla_\delta\theta, \tag{3.7}$$

which is present if there is a soliton in the bulk. Note that we have written $\nabla_\delta\theta$ instead of $\partial_\delta\theta$ which would make Eq. (3.7) differ from Eq. (3.6) by only a surface term since $\varepsilon^{\alpha\beta\gamma\delta}F_{\alpha\beta}\partial_\gamma A_\delta = \varepsilon^{\alpha\beta\gamma\delta}\partial_\gamma(F_{\alpha\beta}A_\delta)$ [66, 67]. However, in Eq. (3.7) the term $\nabla_\delta\theta$ should not be understood as a derivative of something. Because the term (3.6) is not present in the action, the axion field $\nabla_\delta\theta$ in Eq. (3.7) is not a total derivative. Similarly to Sec. 3.1, we introduce a texture of length $2L$ in the bulk by adding a z-dependent mass to the Hamiltonian (3.5)

$$\mathcal{H}_{\text{bulk}} = -2\lambda(\gamma_1\sin k_x + \gamma_2\sin k_y + \gamma_3\sin k_z) + \gamma_0 m_1(k,z) + \gamma_5 m_2(z), \tag{3.8}$$

where now

$$\begin{aligned} m_1(\mathbf{k},z) =& M_1\cos\varphi(z) - 2t(\cos k_x + \cos k_y + \cos k_z)\\ m_2(\mathbf{k},z) =& M_2\sin\varphi(z)\\ \varphi(-L) =& 0,\ \varphi(L) = \pi n. \end{aligned}$$

Again we have broken TRS with the mass term m_2, the symmetry is restored outside the soliton because the TRS breaking mass vanishes. We have parametrized the texture with a smooth function φ, whose value changes from 0 to πn across the interface. The value of N_5 does not depend on the parametrization but only on the boundary values – this was also the case in our previous example, as can be seen in Sec. B.1. Numerical integration of Eq. (3.4) shows that indeed $N_5 = n/2\text{sgn}M_1M_2$, see Fig. 3.3. We will see next that there is a QHE on the $x-y$-plane with a Hall conductance $\sigma_{xy} = e^2N_5/h$. For the simplest possible soliton we have $n = 1$ and σ_{xy} coincides with that obtained from

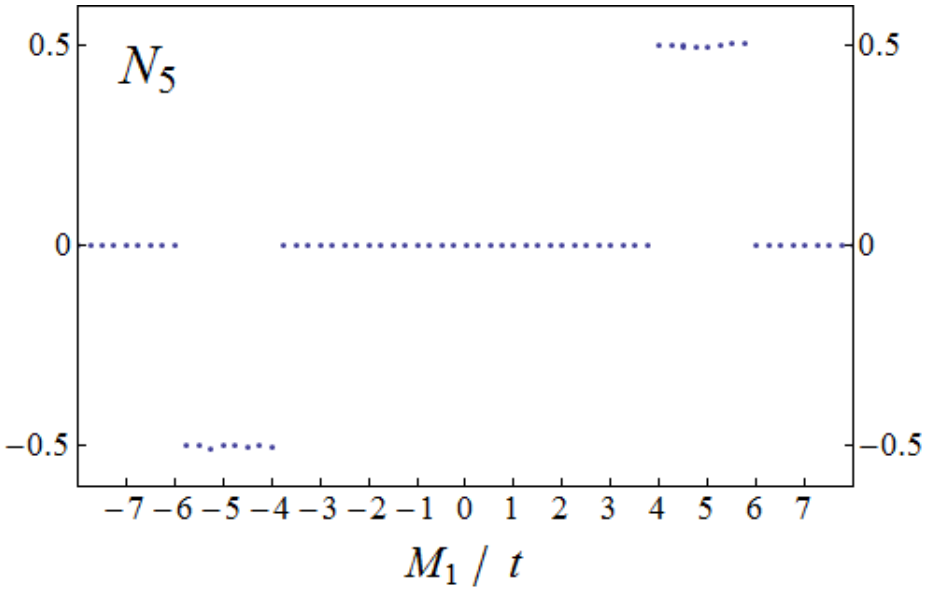

Figure 3.3: A numerical evaluation of the Green function integral N_5 for the model (3.8). The topological quantization of N_5 is clearly seen. The parameters used are $\lambda = t$, $M_2 = 20|M_1|$ and $n = 1$. Numerically it can be observed (not shown) that the z-integration for other values of n just multiplies the plotted value by n.

Eq. (3.6).

3.2.1 The gradient expansion of the axion action

In this subsection we derive the action (3.7) from the gradient expansion and show that it leads to a quantized Hall conductance related to the topological charge N_5 of the soliton. We also show explicitly that the coefficient θ in Eq. (3.6) is zero when constant. This reflects directly the fact that there is no CS forms in odd spatial dimensions.

Let us start from the latter. Instead of expanding the current, it is easier to expand directly the effective action Eq. (B.1) with Eq. (C.7). For the action (3.6) we need to extract the terms proportional to $F_{\alpha\beta}F_{\gamma\delta}$. Only two terms contribute,

$$\begin{aligned} S =& i\mathrm{Tr}\,\ln G = -i\mathrm{Tr}\,\ln G_0^{-1}\left(1 + eG_0A_\alpha\partial_{k_\alpha}G_0^{-1} + \dots\right) \\ =& \text{const.} - i\mathrm{Tr}\sum_{n=1}^{\infty}\frac{1}{n}\left(\cdots + \mathcal{G}_0(G_0^{-1})_F + \mathcal{G}_0(G_0^{-1})_{FF} + \dots\right)^n \\ S_{FF} \equiv& -i\mathrm{Tr}\,\mathcal{G}_0(G_0^{-1})_{FF} - i\mathrm{Tr}\,\frac{1}{2}\mathcal{G}_0(G_0^{-1})_F\mathcal{G}_0(G_0^{-1})_F. \end{aligned}$$

In the second line, we have moved to the Wigner representation allowing a gradient expansion. When we plug in the zeroth order expansion terms $(G_0^{-1})_{F,0}$ and $(G_0^{-1})_{FF,0}$, we obtain

$$\begin{aligned} S_{FF} = &\operatorname{Tr} \frac{e^2}{8} F_{\alpha\beta} F_{\gamma\delta} \partial_{k_\alpha} \mathcal{G}_0 \partial_{k_\beta} \mathcal{G}_0^{-1} \partial_{k_\gamma} \mathcal{G}_0 \partial_{k_\delta} \mathcal{G}_0^{-1} \\ &- \operatorname{Tr} \frac{e^2}{4} F_{\alpha\beta} F_{\gamma\delta} \partial_{k_\gamma} \left(\partial_{k_\delta} \mathcal{G}_0 \partial_{k_\beta} \mathcal{G}_0^{-1} \mathcal{G}_0 \partial_{k_\alpha} \mathcal{G}_0^{-1} \right) \\ &+ \operatorname{Tr} \frac{e^2}{8} F_{\alpha\beta} F_{\gamma\delta} \partial_{k_\gamma} \left(\partial_{k_\beta} \mathcal{G}_0 \partial_{k_\alpha} \partial_{k_\delta} \mathcal{G}_0^{-1} \right). \end{aligned}$$

The last two terms vanish trivially as they are total derivatives in the periodic BZ. The first term can be written in the antisymmetric form

$$\begin{aligned} &\operatorname{Tr} \frac{e^2}{8} F_{\alpha\beta} F_{\gamma\delta} \Lambda_{k_\alpha} \Lambda_{k_\beta} \Lambda_{k_\gamma} \Lambda_{k_\delta} \\ = &\operatorname{Tr} \frac{e^2}{8} \frac{1}{4!} \varepsilon^{\alpha\beta\gamma\delta} F_{\alpha\beta} F_{\gamma\delta} \varepsilon_{\lambda\mu\nu\rho} \Lambda_{k_\lambda} \Lambda_{k_\mu} \Lambda_{k_\nu} \Lambda_{k_\rho}, \end{aligned}$$

which is seen to vanish trivially by moving ρ to the first term inside the trace.

To obtain the S_{AF} term in the action, we start from the current (B.2)

$$j^\gamma = \frac{\delta}{\delta A^\gamma} i \operatorname{Tr} \ln G = ie \int \frac{d^3\mathbf{k} d\omega}{(2\pi)^4} \operatorname{tr} (G^{-1})_W \partial_{k_\gamma} \mathcal{G}, \tag{3.9}$$

The current obtained from the action S_{AF} is first order in the Green function gradients and proportional to the field tensor $F_{\alpha\beta}$. Accordingly, the term we want from the expansion (C.7) is $(G_0^{-1})_{F,1}$. This term is calculated in the Section C.3 of the Appendix C, the result is

$$\begin{aligned} (G_0^{-1})_{F,1} = &\frac{1}{2} e F_{\alpha\beta} \Big\{ \mathcal{G}_0^{-1} \partial_{k_\beta} \mathcal{G}_0 \partial_{k_\alpha} \mathcal{G}_0^{-1} \partial_{[\delta} \mathcal{G}_0 \partial_{k_\delta]} \mathcal{G}_0^{-1} \\ &+ \mathcal{G}_0^{-1} \partial_{[\delta} \mathcal{G}_0 \partial_{k_\delta]} \mathcal{G}_0^{-1} \partial_{k_\beta} \mathcal{G}_0 \partial_{k_\alpha} \mathcal{G}_0^{-1} \\ &- \partial_{[\delta} \mathcal{G}_0^{-1} \partial_{k_\delta]} \left(\partial_{k_\beta} \mathcal{G}_0 \partial_{k_\alpha} \mathcal{G}_0^{-1} \right) \\ &- \partial_{k_\beta} \mathcal{G}_0^{-1} \partial_{k_\alpha} \left(\partial_{[\delta} \mathcal{G}_0 \partial_{k_\delta]} \mathcal{G}_0^{-1} \right) \\ &- \frac{1}{2} \mathcal{G}_0^{-1} \partial_{k_\beta} \partial_{[\delta} \mathcal{G}_0 \partial_{k_\delta]} \partial_{k_\alpha} \mathcal{G}_0^{-1} \Big\} \end{aligned}$$

For most Hamiltonians, such as that of Eq. (3.8), we have $\partial_{k_\alpha} \partial_{k_\beta} \mathcal{G}_0^{-1} = 0$ for all α, β.

The last term vanishes immediately and we have

$$\begin{aligned}(G_0^{-1})_{F,1} =&\frac{1}{4}eF_{\alpha\beta}\mathcal{G}_0^{-1}\left\{\Lambda_{k_\beta}\Lambda_{k_\delta}\Lambda_{k_\alpha}\Lambda_\delta - \Lambda_{k_\beta}\Lambda_\delta\Lambda_{k_\alpha}\Lambda_{k_\delta}\right.\\ &\left.+\Lambda_{k_\delta}\Lambda_{k_\beta}\Lambda_\delta\Lambda_{k_\alpha} - \Lambda_\delta\Lambda_{k_\beta}\Lambda_{k_\delta}\Lambda_{k_\alpha}\right\}.\end{aligned}$$

For $\Lambda_j \equiv \mathcal{G}_0\partial_j\mathcal{G}_0^{-1}$ we have the relation $\partial_i\Lambda_j = \partial_i(\mathcal{G}_0\partial_j\mathcal{G}_0^{-1}) = -\Lambda_i\Lambda_j$. Substitution to the current formula (3.9) leads to the current

$$\begin{aligned}j^\gamma =&\frac{i}{4}e^2F_{\alpha\beta}\int\frac{d^3\mathbf{k}d\omega}{(2\pi)^4}\mathrm{tr}\,\Lambda_{k_\gamma}\left\{\Lambda_{k_\beta}\Lambda_{k_\delta}\Lambda_{k_\alpha}\Lambda_\delta - \Lambda_{k_\beta}\Lambda_\delta\Lambda_{k_\alpha}\Lambda_{k_\delta}\right.\\ &\left.+\Lambda_{k_\delta}\Lambda_{k_\beta}\Lambda_\delta\Lambda_{k_\alpha} - \Lambda_d\Lambda_{k_\beta}\Lambda_{k_\delta}\Lambda_{k_\alpha}\right\}\end{aligned}$$

and to the action

$$\begin{aligned}S =&\frac{i}{8}e^2\mathrm{Tr}\,A_\gamma F_{\alpha\beta}\left\{\Lambda_\delta\Lambda_{k_\beta}\Lambda_{k_\delta}\Lambda_{k_\gamma}\Lambda_{k_\alpha} - \Lambda_\delta\Lambda_{k_\beta}\Lambda_{k_\delta}\Lambda_{k_\alpha}\Lambda_{k_\gamma}\right.\\ &\left.+\Lambda_{k_\delta}\Lambda_{k_\beta}\Lambda_\delta\Lambda_{k_\alpha}\Lambda_{k_\gamma} - \Lambda_{k_\delta}\Lambda_{k_\beta}\Lambda_\delta\Lambda_{k_\gamma}\Lambda_{k_\alpha}\right\},\end{aligned}$$

which is antisymmetric in (α,γ). Let us write the action in a completely antisymmetric form. Because $A_{[\gamma}F_{\alpha]\beta} = -A_{[\alpha}F_{\gamma]\beta} = A_{[\alpha}F_{\beta]\gamma}$, we have

$$\begin{aligned}S =&\frac{i}{4}e^2\mathrm{Tr}\,A_{[\gamma}F_{\alpha]\beta}\\ &\left\{\Lambda_{k_\delta}\Lambda_{k_\beta}\Lambda_\delta\Lambda_{k_\alpha}\Lambda_{k_\gamma} - \Lambda_\delta\Lambda_{k_\beta}\Lambda_{k_\delta}\Lambda_{k_\alpha}\Lambda_{k_\gamma}\right\}\\ =&i\frac{1}{3!}\frac{1}{2}e^2\mathrm{Tr}\,\left(A_{[\gamma}F_{\alpha]\beta} + A_{[\alpha}F_{\beta]\gamma} + A_{[\beta}F_{\gamma]\alpha}\right)\\ &\times\left\{\Lambda_{k_\delta}\Lambda_{k_\beta}\Lambda_\delta\Lambda_{k_\alpha}\Lambda_{k_\gamma} - \Lambda_\delta\Lambda_{k_\beta}\Lambda_{k_\delta}\Lambda_{k_\alpha}\Lambda_{k_\gamma}\right\}\\ =&-ie^2\mathrm{Tr}\,A_{[\alpha}\partial_\beta A_\gamma\Lambda_{d]}\Lambda_{k_\alpha}\Lambda_{k_\beta}\Lambda_{k_\gamma}\Lambda_{k_\delta}\\ =&\frac{e^2}{2i}\frac{1}{4!}\mathrm{Tr}\,\varepsilon^{\alpha\beta\gamma\delta}\varepsilon_{\lambda\mu\nu\rho}F_{\alpha\beta}A_\gamma\Lambda_\delta\Lambda_{k_\lambda}\Lambda_{k_\mu}\Lambda_{k_\nu}\Lambda_{k_\rho}.\end{aligned}$$

This is exactly the Eq. (3.7) with an "axion derivative"

$$\nabla_\delta\theta = 2\pi\frac{1}{4\pi^3 i}\int d^3\mathbf{k}d\omega\mathrm{tr}\,\Lambda_{[\delta}\Lambda_{k_x}\Lambda_{k_y}\Lambda_{k_z}\Lambda_{\omega]}.$$

As we saw in Sec. 2.4, if A is constant in the z-direction, the action

$$S_{AF} = \frac{e^2}{16\pi^2}\varepsilon^{\alpha\beta\gamma\delta}\int d^3\mathbf{x}dtF_{\alpha\beta}A_\gamma\partial_\delta\theta,$$

leads to a QHE on the $x-y$-plane, with a Hall conductance $\sigma_{xy} = e^2\int dz\partial_z\theta/2\pi h$. Replacing $\partial_z\theta$ by $\nabla_z\theta$ we obtain

$$\sigma_{xy} = \frac{1}{4\pi^3 i}\int dz\int d^3\mathbf{k}d\omega\mathrm{tr}\,\Lambda_{[k_x}\Lambda_{k_y}\Lambda_{k_z}\Lambda_\omega\Lambda_{z]} \equiv e^2N_5/h.$$

As we saw in the previous section, N_5 is quantized to $n/2\mathrm{sgn}M_1M_2$ leading to a QHE on the surface.

3.3 Fermion number fractionalization in 1D

In this final section on solitons, we discuss a domain wall in 1D Dirac model which could for example describe a 2D TI edge. We extend the result of fractional charge carried by the domain wall, which was studied already in 1976 by Jackiw and Rebbi [68]. An equivalent condensed matter setup is the celebrated Su-Schrieffer-Heeger model of polyacetylene [69], in which case the domain wall actually carries an integer charge because the half-integer charge is multiplied by the spin degeneracy factor. These charges have never been observed but might be realizable in 2D topological insulators where a TRS breaking perturbation on the edge opens up a gap and gives a mass to the edge modes [5].

We start from the electromagnetic response described by the TRS Landau-Ginzburg action [5]

$$S_F = \frac{1}{2\pi}\int dxdt\theta\varepsilon^{\alpha\beta}\partial_\alpha A_\beta = \text{boundary term} + \frac{1}{2\pi}\int dxdt\varepsilon^{\alpha\beta}A_\alpha\partial_\beta\theta. \tag{3.10}$$

Even though we have not yet introduced the Hamiltonian, we can start the routine procedure and turn the gradient crank. We expand the action (B.1) to pick up the term $(G^{-1})_{A,1}$:

$$\begin{aligned} S =& -i\mathrm{Tr}\,\ln G_0^{-1}\left(1 + eG_0\partial_{k_\alpha}G_0^{-1}A_\alpha + \dots\right) \\ =& \text{const.} - i\mathrm{Tr}\sum_n\frac{1}{n}\left(eG_0\partial_{k_\alpha}G_0^{-1}A_\alpha + \dots\right)^n, \end{aligned}$$

$$\begin{aligned}
S_A =& -ie\mathrm{Tr}\, A_\alpha \mathcal{G}_0 \partial_{k_\alpha} (G_0^{-1})_{W,1} \\
=& -ie\mathrm{Tr}\, A_\alpha \mathcal{G}_0 \partial_{k_\alpha} \left(-i\mathcal{G}_0^{-1} \partial_{[\beta} \mathcal{G}_0 \partial_{k_\beta]} \mathcal{G}_0^{-1}\right) \\
=& -e\mathrm{Tr}\, A_\alpha \partial_{k_\alpha} \left(\partial_{[\beta} \mathcal{G}_0 \partial_{k_\beta]} \mathcal{G}_0^{-1}\right) \\
&+e\mathrm{Tr}\, A_\alpha \mathcal{G}_0 \partial_{k_\alpha} \mathcal{G}_0^{-1} \partial_{[\beta} \mathcal{G}_0 \partial_{k_\beta]} \mathcal{G}_0^{-1} \\
=& \frac{e}{2\pi} \int dx dt A_\alpha \int \frac{dk_x d\omega}{2\pi} \mathrm{tr}\, \mathcal{G}_0 \partial_{k_\alpha} \mathcal{G}_0^{-1} \partial_{[\beta} \mathcal{G}_0 \partial_{k_\beta]} \mathcal{G}_0^{-1}.
\end{aligned}$$

This action leads to a charge

$$q = \int dx\, j^0 = e \int dx \int \frac{dk_x d\omega}{(2\pi)^2} \mathrm{tr}\, \mathcal{G}_0 \partial_\omega \mathcal{G}_0^{-1} \partial_{[x} \mathcal{G}_0 \partial_{k_x]} \mathcal{G}_0^{-1} = eN_3,$$

where

$$N_3 = \int dx \int \frac{dk_x d\omega}{(2\pi)^2} \mathrm{tr}\, \mathcal{G}_0 \partial_{[\omega} \mathcal{G}_0^{-1} \partial_x \mathcal{G}_0 \partial_{k_x]} \mathcal{G}_0^{-1}.$$

This is a topological invariant written in terms of the Green functions. It does not depend on the details of system and allows generalization for interacting systems. Even though we have not introduced a Hamiltonian, we have shown that the charge carried by the domain wall is given by the invariant N_3. This is a new result.

In the Appendix B, Sec. B.2, we evaluate N_3 for the following two-band massive Dirac model

$$H = \sigma_x k_x + m\left(\sigma_y \sin\varphi(x) + \sigma_z \cos\varphi(x)\right),$$

where $\varphi(-\infty) = 0$ and $\varphi(\infty) = \pi n$. We introduced a TRS breaking mass term inside the soliton and TRS is restored at $\pm\infty$. The calculation shows that N_3 is a half-integer $n/2$. This model describes the boundary of a 2D TI with a TRS breaking perturbation [5].

Chapter 4

Conclusions

In this thesis we have given an overview of the vast topic of topological insulators and introduced the method of gradient expansion. We have with the help of numerous examples shown how the gradient expansion can be employed in a wide range of problems on the novel subject of topological insulators.

We started by introducing the momentum space Berry connection and the Chern numbers. These concepts of modern differential geometry assisted us in understanding the topology of the integer quantum Hall effect in the so-called band theory approach. We also presented another way to think about the integer quantum Hall effect. This was provided by the 2D Chern-Simons electromagnetic field theory. With the gradient expansion, we showed that the coefficient in this action was a topological invariant and actually the same as the one that was obtained from the band theory earlier.

Before moving on to the important 4D counterpart of the quantum Hall effect, we reviewed the periodic table of topological phases in the Altland-Zirnbauer symmetry classes. We found that there are many yet undiscovered topological phases with possible winding number invariants, some of which could be presented as Green function integrals. We also showed that the known winding number invariant of chiral insulators could be written in a much simpler form in terms of the Hamiltonian, which was a new result.

We also saw that through the process of Kaluza-Klein type dimensional reduction, low-dimensional topological phases could be interpreted as descendants of higher-dimensional topological insulators. An important example of this was the 4D electromagnetic Chern-Simons field theory which was seen to generate the effective action for the 3D topological insulator. The idea was to use a 3D magnetoelectric polarizability which lead to a $\mathbb{Z}_2$ classification because of gauge symmetry. As another example of the gradient expansion

in action, we obtained the 4D Chern-Simons field theory using the method.

In the third chapter of the main text, we discussed solitons in topological media. The gradient expansion was seen to provide a systematic and powerful tool for analyzing these objects. We derived completely new and generic results concerning domain walls in insulators, and illustrated these with examples. In 3D we saw that a domain wall or a texture between a topological and trivial insulator produces a half-integer quantum Hall effect with a conductance inherited from the texture. This was generic, and as an example we studied the Rosenberg-Franz model of a 3D topological insulator. In 1D we generalized the result of Jackiw and Rebbi and obtained the soliton charge as a generic Green function integral, making it possible to discuss interacting systems. As an example we calculated the soliton charge for a quantum spin Hall insulator edge.

There are many future possibilities for using the gradient expansion in the study of topological phases. In addition to the examples we presented, the gradient expansion allows one to study higher-dimensional smooth topological solitons such as 2D or 3D *skyrmions*. This is a new direction yet to be explored. Another interesting direction arises from the observation that the gradient expansion uses Green's functions as the starting point. For this reason, the expansion could provide an understanding of interacting systems. In Chapter 1 we concluded that the effects of interactions are a major unsolved problem in the subject. In fact, in the course of writing this thesis, the author found that Gurarie has used the gradient expansion with a motivation to study interacting topological insulators [70].

Bibliography

[1] D. J. Thouless, M. Kohmoto, M. P. Nightingale, and M. den Nijs, Phys. Rev. Lett. **49**, 405 (1982).

[2] X. Wen, Adv. Phys. **44**, 405 (1995), arXiv:cond-mat/9506066.

[3] J. E. Moore and L. Balents, Phys. Rev. B **75**, 121306 (2007).

[4] S. Ryu, J. E. Moore, and A. W. W. Ludwig, ArXiv e-prints (2010), 1010.0936.

[5] X.-L. Qi, T. L. Hughes, and S.-C. Zhang, Phys. Rev. B **78**, 195424 (2008).

[6] M. Z. Hasan and C. L. Kane, Rev. Mod. Phys. **82**, 3045 (2010).

[7] M. Zahid Hasan and J. E. Moore, ArXiv e-prints (2010), 1011.5462.

[8] X. Qi and S. Zhang, ArXiv e-prints (2010), 1008.2026.

[9] G. Toulouse and M. Kleman, J. Phys. Lett. (Paris) **37**, L–149 (1976).

[10] G. E. Volovik and V. P. Mineyev, JETP Lett. **24**, 561 (1976).

[11] N. D. Mermin, Rev. Mod. Phys. **51**, 591 (1979).

[12] K. V. Klitzing, G. Dorda, and M. Pepper, Phys. Rev. Lett. **45**, 494 (1980).

[13] R. B. Laughlin, Phys. Rev. B **23**, 5632 (1981).

[14] J. E. Avron, R. Seiler, and B. Simon, Phys. Rev. Lett. **51**, 51 (1983).

[15] M. Kohmoto, Ann. Phys. **160**, 343 (1985).

[16] C. L. Kane and E. J. Mele, Phys. Rev. Lett. **95**, 146802 (2005).

[17] C. L. Kane and E. J. Mele, Phys. Rev. Lett. **95**, 226801 (2005).

[18] G. E. Volovik and V. M. Yakovenko, J. Phys. C **1**, 5263 (1989).

[19] G. E. Volovik, Phys. Lett. A **128**, 277 (1988).

[20] B. A. Bernevig, T. A. Hughes, and S. C. Zhang, Science **314**, 1757 (2006).

[21] M. König *et al.*, Science **318**, 766 (2007).

[22] L. Fu, C. L. Kane, and E. J. Mele, Phys. Rev. Lett. **98**, 106803 (2007).

[23] R. Roy, Phys. Rev. B **79**, 195322 (2009).

[24] H. B. Nielsen and M. Ninomiya, Phys. Lett. B **130**, 389 (1983).

[25] F. Wilczek, Phys. Rev. Lett. **58**, 1799 (1987).

[26] L. Fu and C. L. Kane, Phys. Rev. B **76**, 045302 (2007).

[27] X.-L. Qi, R. Li, J. Zang, and S.-C. Zhang, Science **323**, 1184 (2009).

[28] G. Rosenberg and M. Franz, Phys. Rev. B **82**, 035105 (2010).

[29] D. Hsieh *et al.*, Nature **452**, 970 (2008).

[30] Y. Xia *et al.*, ArXiv e-prints (2008), 0812.2078.

[31] Y. Xia *et al.*, Nature Physics **5**, 398 (2009).

[32] T. Zhang *et al.*, Phys. Rev. Lett. **103**, 266803 (2009).

[33] D. Hsieh *et al.*, Phys. Rev. Lett. **103**, 146401 (2009).

[34] Y. Xia *et al.*, ArXiv e-prints (2009), 0907.3089.

[35] L. Fu and C. L. Kane, Phys. Rev. Lett. **100**, 096407 (2008).

[36] J. C. Y. Teo and C. L. Kane, Phys. Rev. Lett. **104**, 046401 (2010).

[37] J. Linder, Y. Tanaka, T. Yokoyama, A. Sudbø, and N. Nagaosa, Phys. Rev. Lett. **104**, 067001 (2010).

[38] F. Wilczek, Nature Physics **5**, 614 (2009).

[39] C. Nayak, S. H. Simon, A. Stern, M. Freedman, and S. Das Sarma, Rev. Mod. Phys. **80**, 1083 (2008).

[40] M. Levin and A. Stern, Phys. Rev. Lett. **103**, 196803 (2009).

[41] G. Y. Cho and J. E. Moore, ArXiv e-prints (2010), 1011.3485.

[42] J. Maciejko, X.-L. Qi, A. Karch, and S.-C. Zhang, Phys. Rev. Lett. **105**, 246809 (2010).

[43] B. Swingle, M. Barkeshli, J. McGreevy, and T. Senthil, ArXiv e-prints (2010), 1005.1076.

[44] M. Nakahara, *Geometry, Topology and Physics*, Taylor & Francis Ltd, 2003.

[45] L. D. Landau and E. Lifshitz, *Quantum Mechanics: Non-Relativistic Theory, 3rd Edition*, Butterworth-Heinemann, 1991.

[46] F. Wilczek and A. Zee, Phys. Rev. Lett. **52**, 2111 (1984).

[47] F. D. M. Haldane, Phys. Rev. Lett. **61**, 2015 (1988).

[48] F. D. M. Haldane and E. H. Rezayi, Phys. Rev. B **31**, 2529 (1985).

[49] S.-C. Zhang and J. Hu, Science **294**, 823 (2001).

[50] R. D. King-Smith and D. Vanderbilt, Phys. Rev. B **47**, 1651 (1993).

[51] G. Ortiz and R. M. Martin, Phys. Rev. B **49**, 14202 (1994).

[52] S. C. Zhang, Int. J. Mod. Phys. B **6**, 25 (1992).

[53] A. Schnyder, S. Ryu, A. Furusaki, and A. Ludwig, Phys. Rev. B **78**, 195125 (2008).

[54] S. Ryu, A. P. Schnyder, A. Furusaki, and A. W. W. Ludwig, New J. Phys. **12**, 065010 (2010).

[55] L. Fu, Phys. Rev. Lett. **106**, 106802 (2011).

[56] M. R. Zirnbauer, J. Math. Phys. **37**, 4986 (1996).

[57] A. Altland and M. R. Zirnbauer, Phys. Rev. B **55**, 1142 (1997).

[58] M. L. Mehta, *Random matrices*, Elsevier/Academic Press, 2004.

[59] G. E. Volovik, *The Universe in a Helium Droplet*, Oxford University Press, New York, 2003.

[60] T. Vachaspati, *Kinks and Domain Walls: An Introduction to Classical and Quantum Solitons*, Cambridge University Press, 2006.

[61] V. P. Mineyev and G. E. Volovik, Phys. Rev. B **18**, 3197 (1978).

[62] G. E. Volovik, JETP Lett. **28**, 59 (1978).

[63] N. Steenrod, *The topology of fibre bundles*, University Press, Princeton, NJ, 1951.

[64] J. I. Väyrynen and G. E. Volovik, JETP Lett. **63**, 378 (2011).

[65] K. Chen and P. A. Lee, ArXiv e-prints (2010), 1012.2084.

[66] M. M. Vazifeh and M. Franz, Phys. Rev. B **82**, 233103 (2010).

[67] A. M. Essin, J. E. Moore, and D. Vanderbilt, Phys. Rev. Lett. **102**, 146805 (2009).

[68] R. Jackiw and C. Rebbi, Phys. Rev. D **13**, 3398 (1976).

[69] W. P. Su, J. R. Schrieffer, and A. J. Heeger, Phys. Rev. Lett. **42**, 1698 (1979).

[70] V. Gurarie, Phys. Rev. B **83**, 085426 (2011).

[71] A. Altland and B. Simons, *Condensed Matter Field Theory*, Cambridge University Press, Oxford, 2004.

[72] A. Cortijo, A. G. Grushin, and M. A. H. Vozmediano, Phys. Rev. B **82**, 195438 (2010).

[73] C. Gorini, P. Schwab, R. Raimondi, and A. L. Shelankov, Phys. Rev. B **82**, 195316 (2010).

[74] M. K. Weigel, S. Haddad, and F. Weber, J. Phys. G **17**, 619 (1991).

[75] J. W. Serene and D. Rainer, Phys. Rep. **101**, 221 (1983).

[76] G. E. Volovik, JETP Lett. **67**, 1804 (1988).

[77] M. Khalkhali and M. Marcolli, *An invitation to noncommutative geometry*, World Scientific, 2008.

Appendix A

Kubo formula

In this appendix, we derive the Kubo formula for conductivity using first order perturbation theory. A perturbing external electric field is introduced and the resulting current calculated.

Consider a system in a periodic perturbation $\hat{V}e^{-i\omega t}+\hat{V}^\dagger e^{i\omega t}$. We seek to calculate the matrix element $f_{nm} = \int d^2\mathbf{x}\psi_n^*(\mathbf{x})\hat{f}(\mathbf{x})\psi_m(\mathbf{x})$ of a single-particle operator $\hat{f}$. To linear order we can write $f_{nm} = f_{nm}^{(0)} + f_{nm}^{(1)}$ where $f_{nm}^{(0)}$ is the matrix element for an unperturbed system and $f_{nm}^{(1)}$ is the first order change. The diagonal matrix element $f_{nn}^{(1)}$ can be written in terms of V_{nm} and $f_{nm}^{(0)}$ [45]:

$$f_{nn}^{(1)}(t) = f_{nn}^{(0)} - \sum_{m\neq n}\left\{e^{-i\omega t}\left[\frac{f_{nm}^{(0)}V_{mn}}{\omega_{mn}-\omega}+\frac{f_{mn}^{(0)}V_{nm}}{\omega_{mn}+\omega}\right]+e^{i\omega t}\left[\frac{f_{nm}^{(0)}V_{nm}^*}{\omega_{mn}+\omega}+\frac{f_{mn}^{(0)}V_{mn}^*}{\omega_{mn}-\omega}\right]\right\}, \tag{A.1}$$

where $\omega_{mn} = E_m - E_n$. The many-body operator corresponding to $\hat{f}$ is $\hat{F} = \sum_i \hat{f}(\mathbf{x}_i) = \sum_{m,n} f_{mn}\hat{c}_m^\dagger\hat{c}_n$ and we shall use the bracket notation $f_{mn} \equiv \langle m|\hat{f}|n\rangle$. The expectation value of $\hat{F}$ is thus $\left\langle \hat{F}(t)\right\rangle = \sum_m f_{mm}n_m$ where $n_m = n_F(E_m)$ is the Fermi distribution function when we use an energy eigenbasis. We consider the zero temperature case where the Fermi distribution becomes a step function, $n_F(E_n) = \theta(E_n - E_F)$. At zero temperature we have

$$\left\langle \hat{F}(t)\right\rangle = \sum_{\mathbf{k},n}\theta(E_n(\mathbf{k})-E_F)f_{\mathbf{k},nn}(t) = A\int\frac{d^2\mathbf{k}}{(2\pi)^2}\sum_n\theta(E_n-E_F)f_{nn}(t),$$

where A is the area of the sample.

Now we leave the general considerations and discuss the quantum Hall system. The Bloch Hamiltonian is

$$\mathcal{H}_{\mathbf{k}}(x,y) = \frac{1}{2m}(-i\nabla + \mathbf{k} + e\mathbf{A})^2 + U(x,y). \tag{A.2}$$

In a linear approximation the interaction Hamiltonian is $\hat{V} = e\hat{\mathbf{v}} \cdot \mathbf{A}$, where $\hat{v} = \hat{p}/m$ is the single-particle velocity operator. To obtain the conductance, we need the one-particle current density operator $\hat{\mathbf{j}}$. Its matrix elements are

$$j^i_{mn} = -\frac{e}{2mA}\left(\langle m,\mathbf{k}|\hat{p}^i|n,\mathbf{k}\rangle + \langle n,\mathbf{k}|\hat{p}^i|m,\mathbf{k}\rangle^*\right) = -\frac{e}{2A}(v^i_{mn} + v^{*i}_{nm}),$$

where $i = 1,2$ in 2D. We use an orthogonal energy eigenbasis labeled by the band index and momentum, $\mathcal{H}_{\mathbf{k}}|n,\mathbf{k}\rangle = E_n(\mathbf{k})|n,\mathbf{k}\rangle$. For the Bloch Hamiltonian (A.2) the off-diagonal matrix elements of the velocity can be written as

$$\begin{aligned} v^i_{mn} =& (\partial_{k_i}\mathcal{H}_{\mathbf{k}})_{mn} = \omega_{nm}\langle m,\mathbf{k}|\partial_{k_i}|n,\mathbf{k}\rangle \\ =& \omega_{mn}(\partial_{k_i}\langle m,\mathbf{k}|)|n,\mathbf{k}\rangle = \omega_{mn}\langle n,\mathbf{k}|\partial_{k_i}|m,\mathbf{k}\rangle^* = v^{i*}_{nm} \\ j^i_{mn} =& -\frac{e}{A}v^i_{mn} = j^{i*}_{nm}. \end{aligned}$$

Let us now consider an external electric field $\mathbf{E}(t) = \mathbf{E}_\omega(e^{i\omega t} + e^{-i\omega t})$ corresponding to a vector potential $\mathbf{A}(t) = \frac{i}{\omega}\mathbf{E}_\omega(e^{i\omega t} - e^{-i\omega t})$. In Eq. (A.1) we sum over off-diagonal matrix elements, substituting the current we get

$$\begin{aligned} j^i_{nn}(t) =& -\frac{e}{A}\sum_{m\neq n}\left\{e^{-i\omega t}\left[\frac{j^{(0)i}_{nm}v^j_{mn}}{\omega_{mn}-\omega} + \frac{j^{(0)i}_{mn}v^j_{nm}}{\omega_{mn}+\omega}\right] + e^{i\omega t}\left[\frac{j^{(0)i}_{nm}v^{*j}_{mn}}{\omega_{mn}+\omega} + \frac{j^{(0)i}_{mn}v^{*j}_{nm}}{\omega_{mn}-\omega}\right]\right\}A^j \\ =& \frac{ie}{A\omega}\sum_{m\neq n}\left\{e^{-i\omega t}\left[\frac{j^{(0)i}_{nm}v^j_{mn}}{\omega_{mn}-\omega} + \frac{j^{(0)\alpha}_{mn}v^j_{nm}}{\omega_{mn}+\omega}\right] + e^{i\omega t}\left[\frac{j^{(0)i}_{nm}v^{*j}_{mn}}{\omega_{mn}+\omega} + \frac{j^{(0)i}_{mn}v^{*j}_{nm}}{\omega_{mn}-\omega}\right]\right\}E^j_\omega \\ =& \frac{e^2}{iA\omega}\sum_{m\neq n}\left\{e^{-i\omega t}\left[\frac{v^i_{nm}v^j_{mn}}{\omega_{mn}-\omega} + \frac{v^j_{nm}v^i_{mn}}{\omega_{mn}+\omega}\right] + e^{i\omega t}\left[\frac{v^i_{nm}v^j_{mn}}{\omega_{mn}-\omega} + \frac{v^j_{nm}v^i_{mn}}{\omega_{mn}+\omega}\right]^*\right\}E^j_\omega. \end{aligned}$$

Writing $\mathbf{j}_{nn}(t) = \mathbf{j}_{nn}(\omega)e^{-i\omega t} + \text{c.c.}$, we have the frequency representation

$$j^i_{nn}(\omega) = \frac{e^2}{iA\omega}\sum_{m\neq n}\left[\frac{v^i_{nm}v^j_{mn}}{\omega_{mn}-\omega} + \frac{v^j_{nm}v^i_{mn}}{\omega_{mn}+\omega}\right]E^j_\omega = \sigma^{(n)}_{ij}(\omega)E^j_\omega \tag{A.3}$$

for a single band. The total conductance is the sum over bands, weighted with the occupation numbers,

$$\begin{aligned}\sigma_{xy}(\omega) =& \frac{e^2}{i\omega}\int \frac{d^2\mathbf{k}}{(2\pi)^2}\sum_{n,m\neq n} n_F(E_n)\left[\frac{v^x_{nm}v^y_{mn}}{\omega_{mn}-\omega}+\frac{v^y_{nm}v^x_{mn}}{\omega_{mn}+\omega}\right]\\ =& \frac{e^2}{i\omega}\int \frac{d^2\mathbf{k}}{(2\pi)^2}\sum_{n,m\neq n} \theta(E_n-E_F)\left[\frac{(\partial_{k_x}\mathcal{H}_\mathbf{k})_{nm}(\partial_{k_y}\mathcal{H}_\mathbf{k})_{mn}}{\omega_{mn}-\omega}+\frac{(\partial_{k_x}\mathcal{H}_\mathbf{k})_{mn}(\partial_{k_y}\mathcal{H}_\mathbf{k})_{nm}}{\omega_{mn}+\omega}\right].\end{aligned}$$

For a stationary electric field we have a DC response

$$\begin{aligned}\sigma_{xy} =& \lim_{\omega\to 0}\int \frac{d^2\mathbf{k}}{(2\pi)^2}\sum_{n,m\neq n}\frac{e^2}{i}\left[\theta(E_n-E_F)\frac{(\partial_{k_x}\mathcal{H}_\mathbf{k})_{nm}(\partial_{k_y}\mathcal{H}_\mathbf{k})_{mn}}{\omega_{mn}}(\frac{1}{\omega_{mn}}+\frac{1}{\omega})\right.\\ &\left.-\theta(E_m-E_F)\frac{(\partial_{k_x}\mathcal{H}_\mathbf{k})_{nm}(\partial_{k_y}\mathcal{H}_\mathbf{k})_{mn}}{\omega_{mn}}(\frac{1}{\omega_{mn}}-\frac{1}{\omega})\right]\\ =& \int \frac{d^2\mathbf{k}}{(2\pi)^2}\sum_{n,m\neq n}\frac{e^2}{i}\frac{(\partial_{k_x}\mathcal{H}_\mathbf{k})_{nm}(\partial_{k_y}\mathcal{H}_\mathbf{k})_{mn}}{\omega^2_{mn}}\left(\theta(E_n-E_F)-\theta(E_m-E_F)\right)\\ =& ie^2\int \frac{d^2\mathbf{k}}{(2\pi)^2}\sum_{n\in\text{occ.}}\sum_{m\in\text{unocc.}}\varepsilon^{ij}\frac{(\partial_{k_i}\mathcal{H}_\mathbf{k})_{nm}(\partial_{k_j}\mathcal{H}_\mathbf{k})_{mn}}{(E_n-E_m)^2},\end{aligned}$$

where in the first equality the divergent-looking $1/\omega$ terms actually vanish: using the identity $(\partial_{k_i}\mathcal{H}_\mathbf{k})_{nm}=\omega_{mn}\langle n,\mathbf{k}|\partial_{k_i}|m,\mathbf{k}\rangle$, the $1/\omega$ part becomes

$$\begin{aligned}&\sum_{n,m} ie^2\frac{(\partial_{k_i}\mathcal{H}_\mathbf{k})_{nm}(\partial_{k_j}\mathcal{H}_\mathbf{k})_{mn}-(\partial_{k_i}\mathcal{H}_\mathbf{k})_{mn}(\partial_{k_j}\mathcal{H}_\mathbf{k})_{nm}}{\omega_{mn}\omega}\theta(E_n-E_F)\\ =&\sum_{n,m} ie^2\theta(E_n-E_F)\frac{\langle n,\mathbf{k}|\partial_{k_i}|m,\mathbf{k}\rangle\langle m,\mathbf{k}|\partial_{k_j}\mathcal{H}_\mathbf{k}|n,\mathbf{k}\rangle-\langle n,\mathbf{k}|\partial_{k_j}|m,\mathbf{k}\rangle\langle m,\mathbf{k}|\partial_{k_i}\mathcal{H}_\mathbf{k}|n,\mathbf{k}\rangle}{\omega}\\ =&\sum_{n} ie^2\theta(E_n-E_F)\frac{\langle n,\mathbf{k}|\partial_{k_i}\partial_{k_j}\mathcal{H}_\mathbf{k}-\partial_{k_j}\partial_{k_i}\mathcal{H}_\mathbf{k}|n,\mathbf{k}\rangle}{\omega}=0.\end{aligned}$$

For completeness, we give the single band conductance calculated from Eq. (A.3)

$$\sigma^{(n)}_{\alpha\beta} = \frac{e^2}{i}\int\frac{d^2\mathbf{k}}{(2\pi)^2}\sum_m \varepsilon^{ij}\langle n,\mathbf{k}|\partial_{k_i}|m,\mathbf{k}\rangle\langle m,\mathbf{k}|\partial_{k_j}|n,\mathbf{k}\rangle. \tag{A.4}$$

Appendix B

Green's functions and Green function invariants

In this appendix we recall the basic facts of imaginary time Green's functions and path integrals. This way we also explain our notation. In Secs. B.1 and B.2 we evaluate the topological invariants N_3 and N_5 presented in the main text.

Consider a generic single-particle Hamiltonian in d spatial dimensions,

$$H = \sum_{\alpha\beta} \int d^d\mathbf{x}_1 \int d^d\mathbf{x}_2 \psi^\dagger_\alpha(\mathbf{x}_1) \left(\mathcal{H}_{\alpha\beta}(\mathbf{x}_1,\mathbf{x}_2) - \delta_{\alpha\beta}\delta(\mathbf{x}_1,\mathbf{x}_2)\mu\mathcal{N}\right) \psi_\beta(\mathbf{x}_2).$$

Throughout this thesis we have set the chemical potential, or Fermi energy to zero: $\mu = E_F = 0$. This loses the term $\mu\mathcal{N}$ in the previous equation.

The Matsubara (or imaginary time) Green function is defined as [71]

$$G_{\alpha_1\alpha_2}(x_1,x_2) = -\left\langle T_\tau \psi_{\alpha_1}(x_1)\psi^\dagger_{\alpha_2}(x_2)\right\rangle,$$

where $x_i \equiv (\mathbf{x}_i,\tau_i)$ and the metric is Euclidean. We will from now on suppress the indices α_i and understand objects with two indices as matrices. In this notation, all Kronecker deltas will correspond to unit matrices $\delta_{\alpha\beta} \to 1$.

Taking the τ-derivative yields $\delta(x_1,x_2) = \int d^{d+1}x_3 \left(-\delta(x_1,x_3)\partial_{\tau_3} - \mathcal{H}(x_1,x_3)\right) G(x_3,x_2)$ or

$$G^{-1}(x_1,x_2) = -\delta(x_1,x_2)\partial_{\tau_1} - \mathcal{H}(x_1,x_2)$$

with appropriate boundary conditions.

Coupled to an external field A, the system is described with the path integral

$$Z = \int \mathcal{D}A\mathcal{D}\psi^\dagger\mathcal{D}\psi e^{-S^E[A,\psi,\psi^\dagger]-S^E[A]},$$

where $S[A]$ is the free field action. We can separate the fermionic path integral

$$Z[A] = \int \mathcal{D}\psi^\dagger\mathcal{D}\psi e^{-S[A,\psi,\psi^\dagger]},$$

and define the *effective action*

$$S^E_{eff}[A] = -\ln Z[A],$$

which is obtained by integrating out the fermions. We are not interested in the dynamics of the field A and do not include the term $S^E[A]$ in the effective action. By calculating the fermionic integral, we can obtain an expression for $Z[A]$ in terms of the fermion Green function G, as is shown below. The Euclidean action for the fermions is [71]

$$S^E[\psi,\psi^\dagger] = \int d^d\mathbf{x}_1 \int d^d\mathbf{x}_2 \int_0^\beta d\tau \psi^\dagger_\tau(\mathbf{x}_1)\left[\delta(x_1,x_2)\partial_\tau + \mathcal{H}(\mathbf{x}_1,\mathbf{x}_2)\right]\psi_\tau(\mathbf{x}_2).$$

Let us at this point move to zero temperature and set $\beta \to \infty$. Substituting the Fourier transformed field operators,

$$\psi_\tau = \int \frac{d\omega}{2\pi}\psi_\omega e^{-i\omega\tau}$$
$$\psi^\dagger_\tau = \int \frac{d\omega}{2\pi}\psi^\dagger_\omega e^{i\omega\tau}$$

to the action gives the frequency representation

$$S^E[\psi^\dagger,\psi] = \int d^d\mathbf{x}_1 \int d^d\mathbf{x}_2 \int \frac{d\omega}{2\pi}\psi^\dagger_\omega(\mathbf{x}_1)\left[-i\delta(\mathbf{x}_1,\mathbf{x}_2)\omega + \mathcal{H}(\mathbf{x}_1,\mathbf{x}_2)\right]\psi_\omega(\mathbf{x}_2).$$

The integral $Z[A]$ is Gaussian:

$$Z[A] = \det\left[i(\omega + eA_0) - \mathcal{H}(\mathbf{x}_1,\mathbf{x}_2)\right].$$

Using the trace-log formula $\det K = \exp \mathrm{Tr}\, \ln K$ we can write the effective action as

$$S^E_{eff}[A] = \int d^{d+1}x_1 \mathrm{tr}\, \ln G(A; x_1, x_1),$$

in terms of the Green function $G = (i\omega - \mathcal{H})^{-1}$. We can move to real time by setting $\tau = it$ and obtain

$$S_{eff}[A] = i\mathrm{Tr}\, \ln G(A). \tag{B.1}$$

$$j^\gamma = \frac{\delta}{\delta A_\gamma} S_{eff} \tag{B.2}$$

The Eqs. (B.1) and (B.2) are constantly used in this thesis. We will apply the gradient expansion to these equations. There are also different methods to expand the action (B.1) [72].

We obtain a useful representation for the Green function when $\mathcal{H}$ is expanded in its orthonormal eigenbasis. In this case we have $\mathcal{H} = \sum_n E_n |n\rangle\langle n|$ which allows us to write

$$G = \sum_n \frac{|n\rangle\langle n|}{i\omega - E_n}.$$

The validity of this can be easily checked by evaluating GG^{-1}. With this representation one can show the equivalence between the Chern numbers introduced in Sec. 1.2 and the Green function invariants of Subsec. 1.3.2 and Sec. 2.5. This is seen from the form of the momentum space Berry connection $\mathcal{A}_i^{mn} = \langle m| \partial_{k_i} |n\rangle$. The frequency integral in the Green function invariants gives conditions for the band indices $m, n, \ldots$. In Subsec. 1.3.2, the calculation is shown for the first Chern number C_1.

B.1 Evaluation of N_5 for a massive Dirac model

In this section we evaluate the invariant

$$N_5 = \frac{1}{4\pi^3 i} \int dz \int d^3\mathbf{k} d\omega \mathrm{tr}\, \mathcal{G}\partial_{[k_x}\mathcal{G}^{-1}\mathcal{G}\partial_{k_y}\mathcal{G}^{-1}\mathcal{G}\partial_{k_z}\mathcal{G}^{-1}\mathcal{G}\partial_\omega\mathcal{G}^{-1}\mathcal{G}\partial_{z]}\mathcal{G}^{-1}$$

for the massive Dirac Hamiltonian

$$H(\mathbf{k}, z) = \boldsymbol{\gamma}\cdot\mathbf{k} + \gamma_0 m_1(z) + \gamma_5 m_2(z).$$

The masses inside the soliton are $m_1(z) = m\cos zn\pi$, and $m_2(z) = \sigma m \sin zn\pi$. From the calculation below it is *a posteriori* easy to see that the trace in N_5 is actually the same as

$$\mathrm{tr}\,\mathcal{G}\partial_{k_x}\mathcal{G}^{-1}\mathcal{G}\partial_{k_y}\mathcal{G}^{-1}\mathcal{G}\partial_{k_z}\mathcal{G}^{-1}\mathcal{G}\partial_{\omega}\mathcal{G}^{-1}\mathcal{G}\partial_z\mathcal{G}^{-1}.$$

Using the anticommutativity and the identity $\mathrm{tr}\,\gamma_0\gamma_i\gamma_j\gamma_k\gamma_5 = 4\varepsilon_{ijk}$ of Euclidean gamma matrices, and keeping in mind that momentum and frequency are integrated over a symmetric interval, we have for distinct i, j and k

$$\begin{aligned}
&\int dz \int d^3\mathbf{k}d\omega \mathrm{tr}\,\mathcal{G}\partial_{k_i}\mathcal{G}^{-1}\mathcal{G}\partial_{k_j}\mathcal{G}^{-1}\mathcal{G}\partial_{k_k}\mathcal{G}^{-1}\mathcal{G}\partial_{\omega}\mathcal{G}^{-1}\mathcal{G}\partial_z\mathcal{G}^{-1}\\
=&\int dz \int d^3\mathbf{k}d\omega \mathrm{tr}\,\frac{2\omega m_1'}{(\omega^2+E^2)^5}\left(i\omega+H\right)\gamma_i\left(i\omega+H\right)\gamma_j\left(i\omega+H\right)\gamma_k H\gamma_0\\
+&i\int dz \int d^3\mathbf{k}d\omega \mathrm{tr}\,\frac{(\omega^2-E^2)m_1'}{(\omega^2+E^2)^5}\left(i\omega+H\right)\gamma_i\left(i\omega+H\right)\gamma_j\left(i\omega+H\right)\gamma_k\gamma_0\\
+&i\int dz \int d^3\mathbf{k}d\omega \mathrm{tr}\,\frac{(\omega^2-E^2)m_2'}{(\omega^2+E^2)^5}\left(i\omega+H\right)\gamma_i\left(i\omega+H\right)\gamma_j\left(i\omega+H\right)\gamma_k\gamma_5\\
+&\int dz \int d^3\mathbf{k}d\omega \mathrm{tr}\,\frac{2\omega m_2'}{(\omega^2+E^2)^5}\left(i\omega+H\right)\gamma_i\left(i\omega+H\right)\gamma_j\left(i\omega+H\right)\gamma_k H\gamma_5\\
=&i\int dz \int d^3\mathbf{k}d\omega \mathrm{tr}\,\frac{\omega^2 m_1' m_2}{(\omega^2+E^2)^5}\gamma_i\gamma_j\gamma_5\gamma_k(-\omega^2+E^2)\gamma_0\\
+&i\int dz \int d^3\mathbf{k}d\omega \mathrm{tr}\,\frac{\omega^2 m_1' m_2}{(\omega^2+E^2)^5}\gamma_i\gamma_5\gamma_j\gamma_k(-\omega^2+E^2)\gamma_0\\
+&i\int dz \int d^3\mathbf{k}d\omega \mathrm{tr}\,\frac{\omega^2 m_1' m_2}{(\omega^2+E^2)^5}\gamma_5\gamma_i\gamma_j\gamma_k(-\omega^2+E^2)\gamma_0\\
-&i\int dz \int d^3k d\omega \mathrm{tr}\,\frac{2\omega^4\left(m_1 m_2' - m_1' m_2\right)}{(\omega^2+E^2)^5}\gamma_i\gamma_j\gamma_k\gamma_0\gamma_5\\
+&i\int dz \int d^3\mathbf{k}d\omega \mathrm{tr}\,\frac{m_1\omega^2 m_2'(-\omega^2+E^2)}{(\omega^2+E^2)^5}\gamma_i\gamma_j\gamma_0\gamma_k\gamma_5\\
+&i\int dz \int d^3\mathbf{k}d\omega \mathrm{tr}\,\frac{(-\omega^2+E^2)m_1\omega^2 m_2'}{(\omega^2+E^2)^5}\gamma_i\gamma_0\gamma_j\gamma_k\gamma_5\\
+&i\int dz \int d^3\mathbf{k}d\omega \mathrm{tr}\,\frac{(-\omega^2+E^2)\omega^2 m_1 m_2'}{(\omega^2+E^2)^5}\gamma_0\gamma_i\gamma_j\gamma_k\gamma_5\\
-&i\int dz \int d^3\mathbf{k}d\omega \mathrm{tr}\,\frac{(-\omega^2+E^2)m_1'}{(\omega^2+E^2)^5}H\gamma_i H\gamma_j H\gamma_k\gamma_0\\
-&i\int dz \int d^3\mathbf{k}d\omega \mathrm{tr}\,\frac{(-\omega^2+E^2)m_2'}{(\omega^2+E^2)^5}H\gamma_i H\gamma_j H\gamma_k\gamma_5
\end{aligned}$$

$$
\begin{aligned}
&+i\int dz\int d^3\mathbf{k}d\omega\mathrm{tr}\,\frac{2\omega^2 m_2'}{(\omega^2+E^2)^5}H\gamma_i\gamma_j H\gamma_k H\gamma_5\\
&+i\int dz\int d^3\mathbf{k}d\omega\mathrm{tr}\,\frac{2\omega^2 m_2'}{(\omega^2+E^2)^5}H\gamma_i H\gamma_j\gamma_k H\gamma_5\\
&+i\int dz\int d^3\mathbf{k}d\omega\mathrm{tr}\,\frac{2\omega^2 m_2'}{(\omega^2+E^2)^5}\gamma_i H\gamma_j H\gamma_k H\gamma_5\\
&+i\int dz\int d^3\mathbf{k}d\omega\mathrm{tr}\,\frac{2\omega^2 m_1'}{(\omega^2+E^2)^5}H\gamma_i\gamma_j H\gamma_k H\gamma_0\\
&+i\int dz\int d^3\mathbf{k}d\omega\mathrm{tr}\,\frac{2\omega^2 m_1'}{(\omega^2+E^2)^5}H\gamma_i H\gamma_j\gamma_k H\gamma_0\\
&+i\int dz\int d^3\mathbf{k}d\omega\mathrm{tr}\,\frac{2\omega^2 m_1'}{(\omega^2+E^2)^5}\gamma_i H\gamma_j H\gamma_k H\gamma_0\\
=&i\int dz\int d^3\mathbf{k}d\omega\mathrm{tr}\,\frac{(m_1m_2'-m_1'm_2)}{(\omega^2+E^2)^4}\omega^2\gamma_0\gamma_i\gamma_j\gamma_k\gamma_5\\
&+i\int dz\int d^3\mathbf{k}d\omega\mathrm{tr}\,\frac{(m_1m_2'-m_1'm_2)}{(\omega^2+E^2)^4}E^2\gamma_0\gamma_i\gamma_j\gamma_k\gamma_5\\
=&4i\varepsilon_{ijk}\int dz\int d^3\mathbf{k}d\omega\frac{(m_1m_2'-m_1'm_2)}{(\omega^2+E^2)^3}.
\end{aligned}
$$

Setting (i,j,k) to $(1,2,3)$ and removing the antisymmetrization in N_5, we obtain

$$
\begin{aligned}
N_5=&\frac{1}{4\pi^3 i}4i\int dz\int d^3\mathbf{k}d\omega\frac{m_1m_2'-m_1'm_2}{(\omega^2+E^2)^3}\\
=&\frac{1}{\pi^3}\frac{3\pi}{8}\int dz\int d^3\mathbf{k}\frac{(m_2'm_1-m_2m_1')}{(\mathbf{k}^2+\omega^2+m_1^2+m_2^2)^{5/2}}\\
=&\frac{3}{8\pi^2}4\pi\int dz\frac{(m_2'm_1-m_2m_1')}{3(m_1^2+m_2^2)}\\
=&\frac{3\sigma}{2\pi}\int_0^{n\pi}d\varphi\frac{1}{3(\cos^2\varphi+\sin^2\varphi)}\\
=&\frac{3\sigma}{2\pi}\frac{\pi n}{3}=\frac{\sigma n}{2}.
\end{aligned}
$$

B.2 Evaluation of N_3 for a massive Dirac model

In this section we evaluate the invariant

$$
N_3=\int dx\int\frac{dk_xd\omega}{(2\pi)^2}\mathrm{tr}\,\mathcal{G}_0\partial_{[\omega}\mathcal{G}_0^{-1}\partial_x\mathcal{G}_0\partial_{k_x]}\mathcal{G}_0^{-1}
$$

for the massive two-band Dirac Hamiltonian

$$H = \sigma_x k_x + m\left(\sigma_y \sin\varphi(x) + \sigma_z \cos\varphi(x)\right)$$

where $\varphi(-\infty) = 0$ and $\varphi(\infty) = \pi n$. We substitute the Green function

$$\mathcal{G}_0 = \frac{1}{i\omega - H} = -\frac{i\omega + H}{\omega^2 + E^2},\ E^2 = k_x^2 + m^2$$

to the invariant formula. The trace over Pauli matrices gives only two terms and the calculation is simple:

$$\begin{aligned}
N_3 =& \int dx \int \frac{dk_x d\omega}{(2\pi)^2} \mathrm{tr}\, \mathcal{G}_0 \partial_\omega \mathcal{G}_0^{-1} \partial_{[x} \mathcal{G}_0 \partial_{k_x]} \mathcal{G}_0^{-1} \\
=& \frac{-1}{2} \int dx \int \frac{dk_x d\omega}{(2\pi)^2} \mathrm{tr}\, \frac{i\omega + H}{(\omega^2 + E^2)} i \left(\partial_{k_x} \frac{i\omega + H}{\omega^2 + E^2} m \partial_x H + \partial_x \frac{i\omega + H}{\omega^2 + E^2} \sigma_x \right) \\
=& \frac{1}{2} \int dx \int \frac{dk_x d\omega}{(2\pi)^2} \mathrm{tr}\, \frac{H}{(\omega^2 + E^2)^2} im \left[\partial_x \left(\sigma_y \sin\varphi(x) + \sigma_z \cos\varphi(x) \right), \sigma_x \right] \\
=& \int d\varphi \int \frac{dk_x d\omega}{(2\pi)^2} \frac{2m^2}{(\omega^2 + E^2)^2} \\
=& \int d\varphi \int \frac{dk_x}{2\pi} \frac{m^2}{2(k_x^2 + m^2)^{3/2}} \\
=& \int d\varphi \frac{1}{2\pi} = \frac{n}{2}.
\end{aligned}$$

Appendix C

The gradient expansion

The gradient expansion of the Green function is a well-known method in transport theory [71, 73, 74]. In Refs. [75, 76, 19, 18] it was used to derive topological invariants in superfluid helium, but without rationalization. We fill this gap and present a detailed derivation in this chapter.

Consider a dynamical quantity depending on two different length scales, for example a quantum mechanical observable f describing system with a characteristic scale of λ_F, the Fermi wave length. If this system is in the (weak or low-energy) influence of an external field varying on a "classical" length scale $\Lambda \gg \lambda_F$, it is intuitively clear that some sort of approximation is justified when one considers the dynamics of the whole system. A certain approximation is obtained in the form of a gradient expansion.

Throughout this chapter we use a notation $x = (t, \mathbf{x})$, $x \cdot k = t\omega - \mathbf{x} \cdot \mathbf{k}$ with Minkowskian metric. We will be in d spatial dimensions.

What one often uses are the Fourier transforms of quantities. In quantum mechanics one is usually most interested in the Green functions of the system, i.e., 2-point correlation functions $\mathcal{G}(x_1, x_2)$ which depend on two space-time points. In a homogeneous system the only dependence in the 2-point function is on the separation $x_1 - x_2 \sim \lambda_F$, allowing one to do Fourier transforms. Next we discuss 2-point correlation functions where the above does not hold but there is also a dependence on $\Lambda \sim x_1 + x_2$. In this case one is bound to define *the Wigner transformation*, which can be understood as a partial Fourier transformation. This transformation leaves the classical length scale Λ untouched.

C.1 The Wigner transformation

In this Section we introduce the basic definition and properties of the Wigner transformation. The Wigner transformation can be thought of as a Fourier transformation on the shorter length scale λ_F. Accordingly, one first introduces the so-called center-of-mass coordinates through the relations

$$\begin{aligned} X = &\quad \frac{x_1 + x_2}{2} \sim \Lambda \\ x = &\quad x_1 - x_2 \sim \lambda_F, \end{aligned} \tag{C.1}$$

where $\sim$ denotes the corresponding length scale. Hence x is understood as a quantum mechanical fluctuation around the classical coordinate value X. Next, one Fourier transforms with respect to x, which defines the Wigner transform $A_W(k, X)$ of an operator $A(x_1, x_2)$:

$$A_W(k, X) = \int d^{d+1}x e^{ik\cdot x} A(X + x/2, X - x/2).$$

From now on, we leave out the arguments. Some observations can be made of the Wigner transformation, namely, it has the following important properties:

1. *Trace invariance,*

$$\mathrm{Tr}\, A \equiv \int d^{d+1}x \mathrm{tr}\, A(x, x) = \int d^{d+1}X \int \frac{d^{d+1}k}{(2\pi)^{d+1}} \mathrm{tr}\, A_W(k, X) \equiv \mathrm{Tr}\, A_W.$$

2. *Non-commutativity with inversion,*

$$(A_W)^{-1} \neq (A^{-1})_W \equiv A_W^{-1},$$

   contrary to what one would expect from a normal Fourier transform.

3. *The Moyal product rule* [71]:

$$(AB)_W = A_W \exp \frac{i}{2} \left(\overleftarrow{\nabla} \cdot \overrightarrow{\partial}_k - \overleftarrow{\partial}_k \cdot \overrightarrow{\nabla} \right) B_W. \tag{C.2}$$

Let us show the first item. The Jacobian for the transformation (C.1) is one and thus by

a direct calculation

$$\begin{aligned}\mathrm{Tr}\, A_W &= \int d^{d+1}X \int \frac{d^{d+1}k}{(2\pi)^{d+1}} \int d^{d+1}x e^{ik\cdot x} \mathrm{tr}\, A(X+x/2, X-x/2) \\ &= \int d^{d+1}x_1 \int d^{d+1}x_2 \delta(x_1-x_2) \mathrm{tr}\, A(x_1,x_2) = \mathrm{Tr}\, A.\end{aligned}$$

Derivation of the last item is lengthy and we shall not include it here. It is sketched for example in the textbook [77]. The Moyal product rule is extremely useful and next we use it to derive the gradient expansion in the next Section. We combine the properties 2. and 3. and derive an expression for the Wigner transform of an inverted operator in terms of the operator's Wigner transforms.

C.2 The gradient expansion

Let us now use the Moyal product rule to derive the gradient expansion. We denote the Wigner transformed Green function with a calligraphic font, $G_W \equiv \mathcal{G}$. We will start by seeking $(G^{-1})_W$ in terms of $\mathcal{G}^{-1}$ and $\mathcal{G}$. The product rule gives

$$1 = (GG^{-1})_W = \mathcal{G} \exp \frac{i}{2}\left(\overleftarrow{\nabla}\cdot\overrightarrow{\partial}_k - \overleftarrow{\partial}_k \cdot \overrightarrow{\nabla}\right)(G^{-1})_W \tag{C.3}$$

We expand $(G^{-1})_W$ in gradients of $\mathcal{G}$ and $\mathcal{G}^{-1}$

$$(G^{-1})_W = (G^{-1})_{W,0} + (G^{-1})_{W,1} + \ldots,$$

where $(G^{-1})_{W,i}$ is ith order in the gradients. In zeroth order Eq. (C.3) gives $(G^{-1})_{W,0} = \mathcal{G}^{-1}$, as expected. Subtracting the zeroth order, Eq. (C.3) gives the first order term

$$(G^{-1})_{W,1} = -\frac{i}{2}\mathcal{G}^{-1}\left(\partial_\alpha \mathcal{G} \partial_{k_\alpha}\mathcal{G}^{-1} - \partial_{k_\alpha}\mathcal{G}\partial_\alpha \mathcal{G}^{-1}\right), \tag{C.4}$$

where we used the differentiation identity $\delta\mathcal{G}^{-1}\mathcal{G} = -\mathcal{G}^{-1}\delta\mathcal{G}$ to commute $\mathcal{G}^{-1}$ to the left. Continuing iteratively, we have the second order term

$$\begin{aligned}(G^{-1})_{W,2} =& -\frac{1}{4}\mathcal{G}^{-1}\partial_\beta\mathcal{G}\partial_{k_\beta}\left[\left(\partial_\alpha\mathcal{G}^{-1}\partial_{k_\alpha}\mathcal{G} - \partial_{k_\alpha}\mathcal{G}^{-1}\partial_\alpha\mathcal{G}\right)\mathcal{G}^{-1}\right] \\ &+\frac{1}{4}\mathcal{G}^{-1}\partial_{k_\beta}\mathcal{G}\partial_\beta\left[\left(\partial_\alpha\mathcal{G}^{-1}\partial_{k_\alpha}\mathcal{G} - \partial_{k_\alpha}\mathcal{G}^{-1}\partial_\alpha\mathcal{G}\right)\mathcal{G}^{-1}\right] \\ &+\frac{1}{8}\mathcal{G}^{-1}\left(\partial_\beta\partial_\alpha\mathcal{G}\partial_{k_\alpha}\partial_{k_\beta}\mathcal{G}^{-1} - 2\partial_{k_\beta}\partial_\alpha\mathcal{G}\partial_{k_\alpha}\partial_\beta\mathcal{G}^{-1} + \partial_{k_\beta}\partial_{k_\alpha}\mathcal{G}\partial_\alpha\partial_\beta\mathcal{G}^{-1}\right)\end{aligned} \tag{C.5}$$

C.3 Gauge field expansions

In the previous section, we expanded $(G^{-1})_W$ in gradients of $\mathcal{G}$. For a system weakly coupled to an external U(1) gauge field A, we can further expand the Green function in A and its gradients. Because of the minimal coupling, we have an expansion

$$\mathcal{G} = \mathcal{G}_0 + eA_c\partial_{k_c}\mathcal{G}_0 + \frac{e^2}{2}A_dA_c\partial_{k_c}\partial_{k_d}\mathcal{G}_0 + \ldots, \tag{C.6}$$

where $\mathcal{G}_0$ is evaluated in zero external field. We will plug this expansion in the Eqs. (C.4) and (C.5) and obtain an expansion

$$(G^{-1})_W = (G_0^{-1})_W + (G_0^{-1})_A + (G_0^{-1})_F + (G_0^{-1})_{AF}\ldots, \tag{C.7}$$

where $(G_0^{-1})_W$ is the gradient series in zero external field, $(G_0^{-1})_A$ is the gradient series linear in A, $(G_0^{-1})_F$ is the gradient series linear in gradients of A etc. Further, we will use notation $(G_0^{-1})_{X,i}$ to denote the ith gradient term in the series $(G_0^{-1})_X$. To illustrate the notation, the term $(G_0^{-1})_{FF,3}$ is overall 5th order in gradients, but two of the gradients hit As while the rest operate on the Green functions.

Every term of the expansion Eq. (C.7) can be systematically calculated by substitution of Eq. (C.6) to the Moyal product Eq. (C.3). In the subsection below we list some of the first expansion terms – mainly those needed in the main text.

One comment has to be made. The object we most often want to expand is the current

$$j^\gamma = i\frac{\delta}{\delta A_\gamma}\mathrm{Tr}\,\ln G = ie\mathrm{tr}\,G^{-1}\partial_{k_\gamma}G.$$

In moving to Wigner picture, the product rule has to be remembered and we must not only expand G^{-1} but also the product $G^{-1}\partial_{k_\gamma}G$ under the trace. Fortunately, however,

it is usually sufficient to just include the first term of the Moyal expansion. This is seen by using a different form of the Moyal product,

$$\begin{aligned}
\mathrm{tr}\,(AB)_W =& \,\mathrm{tr}\, e^{\frac{i}{2}(\nabla_1\cdot\partial_{k_2}-\partial_{k_1}\cdot\nabla_2)} A_W(x_1,k_1)B_W(x_2,k_2)\Big|_{(x_1,k_1)=(x_2,k_2)} \\
=& \mathrm{tr}\, A_W B_W \\
&+\frac{1}{2}\sum_{n=0}^{\infty}\frac{i^n}{n!2^n}\,(\nabla_1\cdot\partial_{k_2}-\partial_{k_1}\cdot\nabla_2)^n \mathrm{tr}\, A_W(x_1,k_1)B_W(x_2,k_2)|_{(x_1,k_1)=(x_2,k_2)} \\
&+\frac{1}{2}\sum_{n=0}^{\infty}\frac{i^n}{n!2^n}\,(\nabla_2\cdot\partial_{k_1}-\partial_{k_2}\cdot\nabla_1)^n \mathrm{tr}\, A_W(x_1,k_1)B_W(x_2,k_2)|_{(x_1,k_1)=(x_2,k_2)} \\
=& \mathrm{tr}\, A_W B_W \\
&+\sum_{n=1}^{\infty}\frac{(-1)^n}{(2n)!4^n}\,(\nabla_1\cdot\partial_{k_2}-\partial_{k_1}\cdot\nabla_2)^{2n} \mathrm{tr}\, A_W(x_1,k_1)B_W(x_2,k_2)\Big|_{(x_1,k_1)=(x_2,k_2)}.
\end{aligned}$$

The second equality is obtained by writing $\mathrm{tr}\, AB = \frac{1}{2}\mathrm{tr}\,[A,B]_+$, which cancels all terms odd in gradients. Thus, we have $\mathrm{tr}\,(AB)_W = \mathrm{tr}\, A_W B_W$ to first order accuracy. This precision is sufficient for all calculations in this thesis.

C.3.1 Low-order expansions of Green functions

Here we give for reference some of the simplest gradient expansion terms. The list below contains all the terms used in this thesis.

C.3.1.1 $(G_0^{-1})_A$ to first order:

$$\begin{aligned}
(G_0^{-1})_{A,0} =& eA_\alpha\partial_{k_\alpha}\mathcal{G}_0^{-1}, \\
(G_0^{-1})_{A,1} =& -ieA_\beta\partial_{k_\beta}\left(\mathcal{G}_0^{-1}\partial_{[\alpha}\mathcal{G}_0\partial_{k_\alpha]}\mathcal{G}_0^{-1}\right).
\end{aligned}$$

C.3.1.2 $(G_0^{-1})_F$ to first order:

$$
\begin{aligned}
(G_0^{-1})_{F,0} =& \frac{i}{2} e F_{\alpha\beta} \mathcal{G}_0^{-1} \partial_{k_\alpha} \mathcal{G}_0 \partial_{k_\beta} \mathcal{G}_0^{-1}, \\
(G_0^{-1})_{F,1} =& \frac{1}{2} e F_{\alpha\beta} \left\{ \mathcal{G}_0^{-1} \partial_{k_\beta} \mathcal{G}_0 \partial_{k_\alpha} \mathcal{G}_0^{-1} \partial_{[\gamma} \mathcal{G}_0 \partial_{k_\gamma]} \mathcal{G}_0^{-1} \right. \\
& + \mathcal{G}_0^{-1} \partial_{[\gamma} \mathcal{G}_0 \partial_{k_\gamma]} \mathcal{G}_0^{-1} \partial_{k_\beta} \mathcal{G}_0 \partial_{k_\alpha} \mathcal{G}_0^{-1} \\
& - \partial_{[\gamma} \mathcal{G}_0^{-1} \partial_{k_\gamma]} \left(\partial_{k_\beta} \mathcal{G}_0 \partial_{k_\alpha} \mathcal{G}_0^{-1} \right) \\
& - \partial_{k_\beta} \mathcal{G}_0^{-1} \partial_{k_\alpha} \left(\partial_{[\gamma} \mathcal{G}_0 \partial_{k_\gamma]} \mathcal{G}_0^{-1} \right) \\
& \left. - \frac{1}{2} \mathcal{G}_0^{-1} \partial_{k_\beta} \partial_{[\gamma} \mathcal{G}_0 \partial_{k_\gamma]} \partial_{k_\alpha} \mathcal{G}_0^{-1} \right\}.
\end{aligned}
$$

C.3.1.3 $(G_0^{-1})_{AA}$ to first order:

$$
\begin{aligned}
(G_0^{-1})_{AA,0} =& \frac{1}{2} e^2 A_\alpha A_\beta \partial_{k_\alpha} \partial_{k_\beta} \mathcal{G}_0^{-1} \\
(G_0^{-1})_{AA,1} =& - e^2 \frac{i}{2} A_\alpha A_\beta \partial_{k_\alpha} \partial_{k_\beta} \left(\mathcal{G}_0^{-1} \partial_{[\gamma} \mathcal{G}_0 \partial_{k_\gamma]} \mathcal{G}_0^{-1} \right).
\end{aligned}
$$

C.3.1.4 $(G_0^{-1})_{AF}$ to zeroth order:

$$
(G_0^{-1})_{AF,0} = \frac{i}{2} e^2 F_{\alpha\beta} A_\gamma \partial_{k_\gamma} \left(\mathcal{G}_0^{-1} \partial_{k_\alpha} \mathcal{G}_0 \partial_{k_\beta} \mathcal{G}_0^{-1} \right).
$$

C.3.1.5 $(G_0^{-1})_{FF}$ to zeroth order:

$$
(G_0^{-1})_{FF} = \frac{-e^2}{4} F_{\alpha\beta} F_{\gamma\delta} \left[\mathcal{G}_0^{-1} \partial_{k_\delta} \mathcal{G}_0 \partial_{k_\gamma} \left(\partial_{k_\beta} \mathcal{G}_0^{-1} \partial_{k_\alpha} \mathcal{G}_0 \mathcal{G}_0^{-1} \right) + \frac{1}{2} \mathcal{G}_0^{-1} \partial_{k_\gamma} \left(\partial_{k_\beta} \mathcal{G}_0 \partial_{k_\alpha} \partial_{k_\delta} \mathcal{G}_0^{-1} \right) \right]
$$